

# New Deep WSDOT Standard Sections Extend Spans of Prestressed Concrete Girders



**Stephen J. Seguirant, P.E.**  
Director of Engineering  
Concrete Technology Corporation  
Tacoma, Washington

---

*This paper discusses the new deep precast, prestressed concrete girder sections that have been adopted as Washington State Department of Transportation (WSDOT) Standards. Members of the Pacific Northwest Precast/Prestressed Concrete Institute, in cooperation with WSDOT and other affected support industries, developed sections that are deeper and will span further than previously available WSDOT Standards. Wider spacings and fewer girder lines can also be used for spans in the range of previous WSDOT Standards. The sections are available in both single-piece, pretensioned and multiple-piece, post-tensioned segmental versions. This paper discusses practical considerations in developing the concrete outline, pretensioned span capabilities, and handling and shipping considerations. An appendix section provides sample handling and shipping calculations for the longest girder section and highest level of pretensioning.*

---

**S**ince the early 1960s, precast, prestressed concrete has been the material of choice for bridge superstructures for the Washington State Department of Transportation (WSDOT). Consequently, WSDOT has many years of experience with the design and use of structurally efficient girder sections. Since 1989, the Pacific Northwest Precast/Prestressed Concrete Institute (PNW/PCI) has met annually with WSDOT to discuss subjects of mutual interest, developing a sense of mutual cooperation. Over this period, WSDOT's Standard Plans and Specifications

have been jointly refined to provide top quality bridge products while simultaneously improving production efficiencies.

At the 1996 meeting, the author proposed that industry and WSDOT jointly develop new girder sections that would be deeper and span further than the standard WSDOT sections available at the time. WSDOT enthusiastically agreed, and asked industry to take the lead in developing the sections. A wide variety of people have been consulted during the development of the sections, including producers, contractors, truckers, aca-

demics, and consulting engineers, as well as WSDOT bridge design, bridge rating, construction and transportation permitting personnel. This process has been very similar to that described by Bardow et al.<sup>1</sup> in the development of the New England Bulb-Tee Girder.

This paper documents the development of WSDOT's new deep precast, prestressed concrete girder sections. "Deep" is defined as depths exceeding those previously available, the deepest of which was a W74MG girder [1865 mm (73.5 in.)]. The new section depths are 2100 and 2400 mm (82.68 and 94.49 in.). This increases the available range of depths in approximate increments of 300 mm (11.81 in.). The sections are detailed in hard metric units. The primary goal of the study was to increase the span range capability of standard prestressed concrete girders, and to improve economy by increasing the allowable girder spacing over previous designs.

Throughout this paper, girders will be described as pretensioned or post-tensioned. Pretensioned girders refer to members that are fabricated, shipped and erected as one piece with pretensioned strands as the only source of the prestressing force. Where applicable, pretensioned girders are more economical than post-tensioned girders.

Post-tensioned girders are fabricated in two or more pieces per span and are subsequently post-tensioned together. The source of the prestressing force in post-tensioned girders may be the post-tensioning tendons acting alone or may be a combination of pretensioned and post-tensioned strands. Many scenarios exist for assembling post-tensioned girders.<sup>2</sup> Due to several considerations (primarily, weight), post-tensioned girders provide a much larger span range than pretensioned girders.

The new girder sections were developed using the latest available technical information, including the 1994 AASHTO LRFD Bridge Design Specifications.<sup>3</sup>

## SECTION DEVELOPMENT

The starting point for the development of the new girder sections was

the NU girder series<sup>4</sup> developed at the University of Nebraska under a PCI-sponsored fellowship. The primary goal of the fellowship was to develop a girder section that is highly efficient in continuous span applications. The resulting girder section featured a relatively wide bottom flange to enhance compressive strength in negative moment regions, and to accommodate a large number of pretensioned strands.

The section also featured a relatively thin and wide top flange. The concrete outline, dimensions, and section properties of the NU girder series are given in Ref. 4.

For the purpose of adapting this girder series as standard WSDOT sections, several modifications were made to the NU girders. The concrete outline, dimensions, and section properties of the new WSDOT sections are shown in

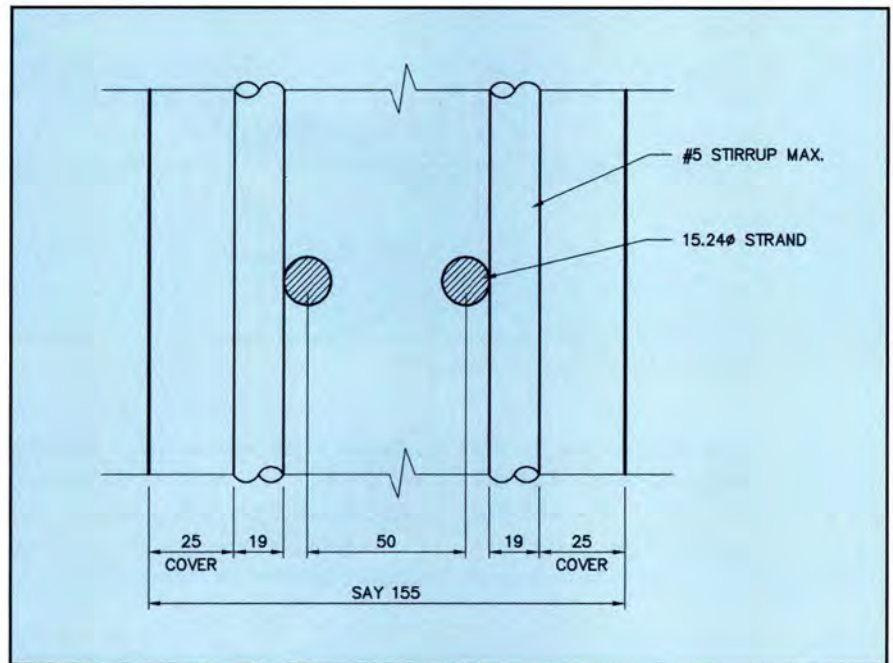


Fig. 1. Pretensioned web configuration.

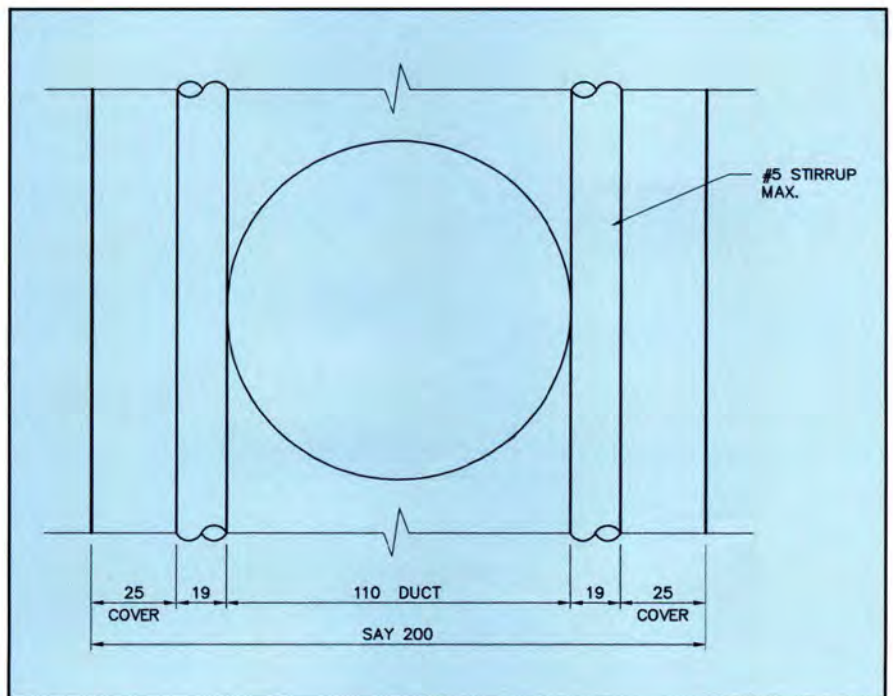


Fig. 2. Post-tensioned web configuration.

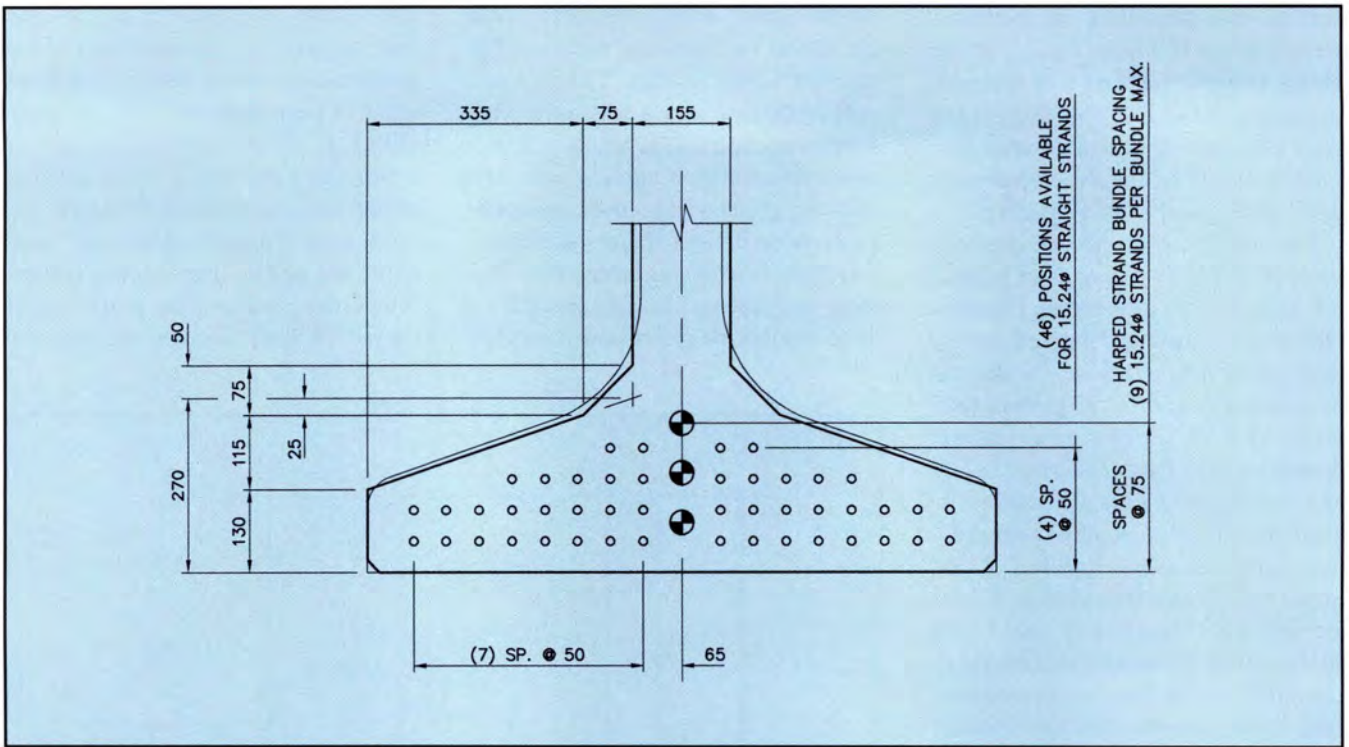


Fig. 3. Pretensioned bottom flange configuration.

Appendix B. The designations for the new pretensioned girders are W21MG and W24MG for the 2100 and 2400 mm (82.68 and 94.49 in.) deep sections, respectively. The post-tensioned

versions of the sections are called the W21PTMG and W24PTMG girders. Modifications to the NU girders, and the reasons for those modifications, are discussed in the following sections.

### General Modifications

As can be seen in Ref. 4, the NU girder series has curved surfaces at both the flange edges and the flange/web junctures. The intent of the curved surfaces is to improve aesthetics and to facilitate placement and consolidation of concrete in the wide bottom flange. Discussions with form fabricators indicated that forms would be somewhat easier to fabricate with sharp breaks at the flange edges and with fillets in lieu of curved surfaces at the flange/web junctures. In particular, transitions from end blocks to web sections in some post-tensioned applications would be easier to accommodate.

Most importantly, WSDOT expressed a preference for sharp edges and fillets in lieu of the curved surfaces. Accordingly, sharp edges and fillets have been detailed into the new sections, as shown in Appendix B. It is anticipated that the fillet at the juncture of the bottom flange and web will facilitate concrete placement and consolidation in a manner similar to the curved surface of the NU girder.

### Web Width

For pretensioned girders, a web width of 155 mm (6.10 in.) was chosen for the new sections in lieu of 150

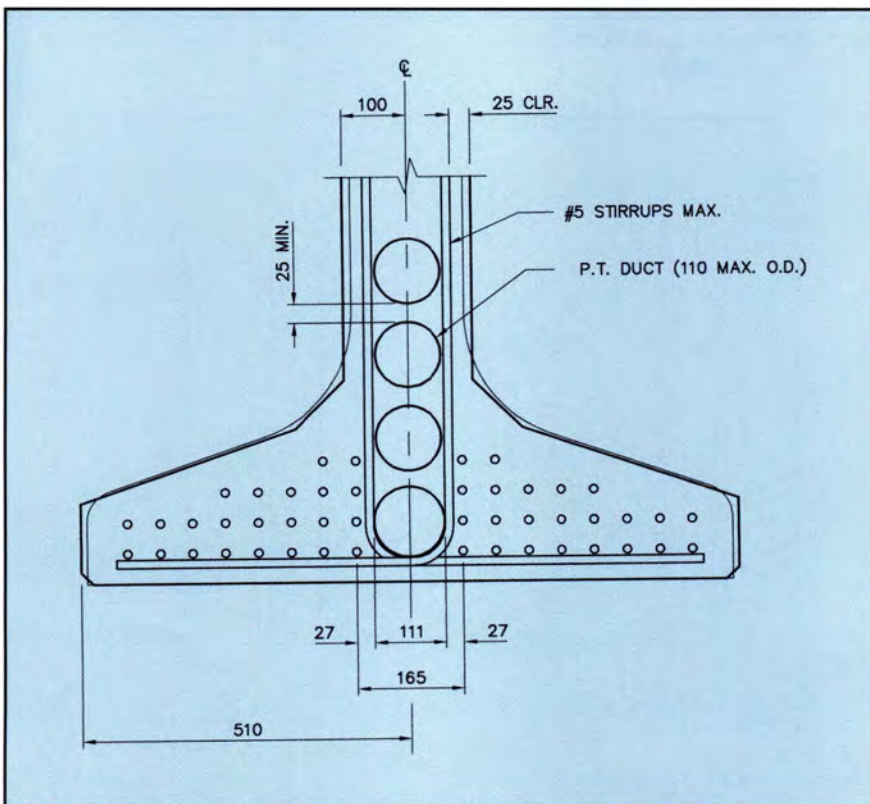


Fig. 4. Post-tensioned bottom flange configuration.

mm (5.91 in.) for the NU girders. This was derived as shown in Fig. 1. This width allows for 15.24 mm (0.60 in.) diameter harped strands on 50 mm (1.97 in.) centers, #5 stirrups, and 25 mm (0.98 in.) of concrete cover.

For post-tensioned girders, a web width of 200 mm (7.87 in.) was chosen for the new sections in lieu of 175 mm (6.89 in.) for the NU girders. This was derived as shown in Fig. 2. The 110 mm (4.33 in.) duct size accommodates commercially available post-tensioning systems of up to nineteen 15.24 mm (0.60 in.) diameter strands per tendon, or twenty-nine 12.70 mm (0.50 in.) strands per tendon.

Also, the clear distance between the duct and form side is 45 mm (1.77 in.), which is more than twice the

maximum aggregate size of 19 mm (0.75 in.). ACI 318-95<sup>s</sup> requires a clear distance between obstructions of at least 1.33 times the maximum aggregate size. With the type of external vibration commonly used on these forms, consolidation of concrete below and around the ducts is not anticipated to be a problem.

### Bottom Flange

The bottom flange of the new girder is shown in Fig. 3 for pretensioned sections and in Fig. 4 for post-tensioned girders. The WSDOT section is shown in heavy lines while the NU section is shown in thin lines. The WSDOT configuration is 5 mm (0.20 in.) thinner than the NU girder series,

has chamfered bottom edges, sharp top edges, and a 75 mm (2.95 in.) fillet in lieu of the curved juncture between the flange and web. Although this configuration is slightly thinner than the NU girder, it still provides more than adequate cover over the strand and mild steel reinforcement. This small decrease in the bottom flange thickness was done primarily as a weight saving measure. With the extended lengths of the pretensioned sections, small increases in weight per unit length add up quickly.

### Top Flange

The top flange of the new girder is shown in Fig. 5 for pretensioned sections, and in Fig. 6 for post-tensioned

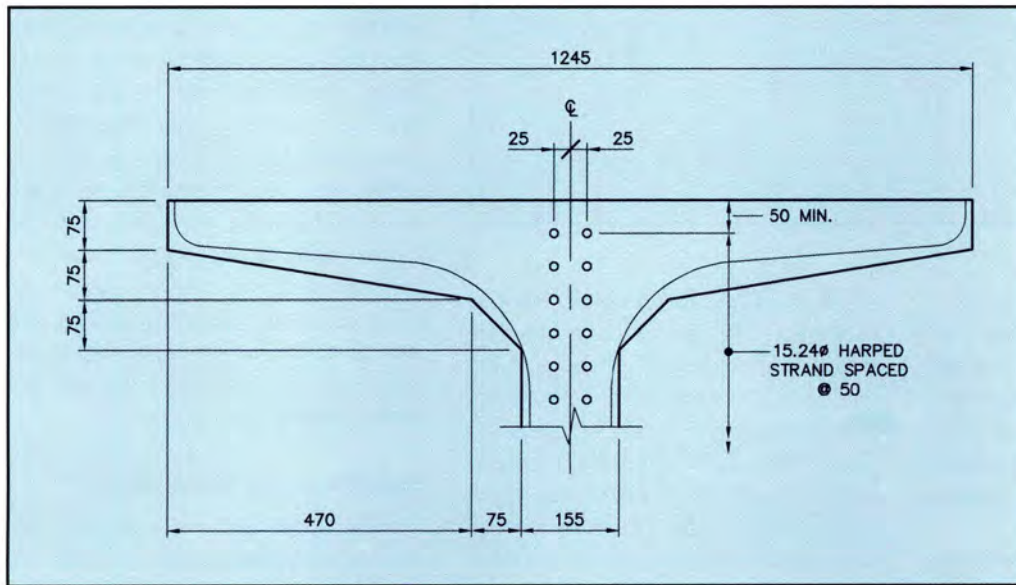


Fig. 5. Pretensioned top flange configuration.

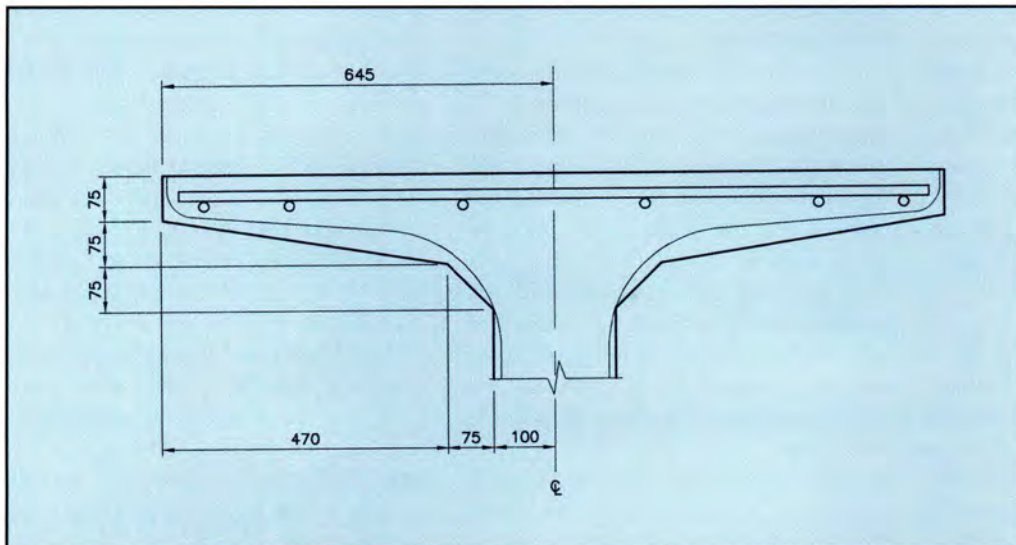


Fig. 6. Post-tensioned top flange configuration.

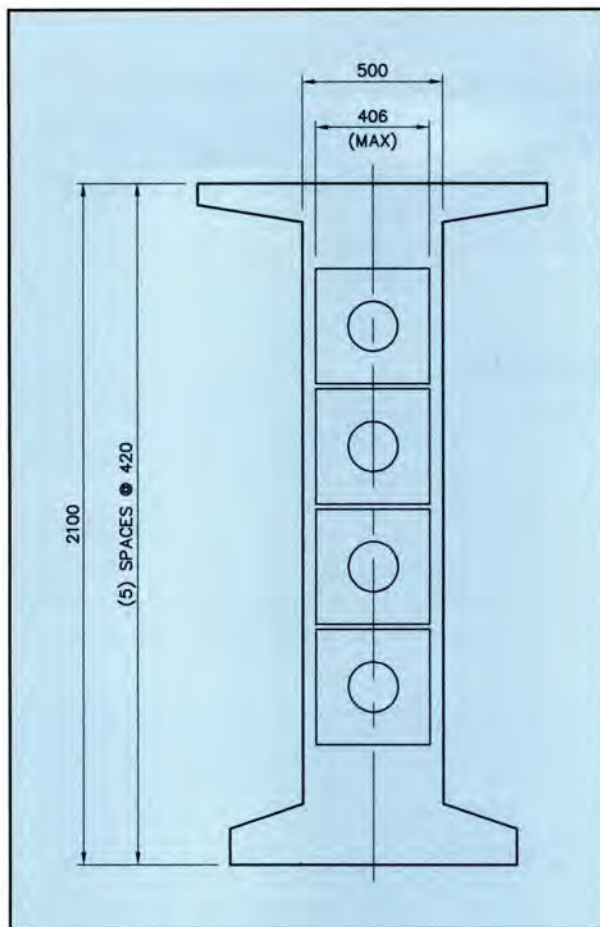


Fig. 7.  
Post-tensioned end block  
configuration.

girders. Again, the WSDOT section is shown in heavy lines while the NU section is shown in thin lines. Both the top and bottom flange edges of the new sections are sharp, and again a 75 mm (2.95 in.) fillet replaces the curved juncture between the flange and web.

The flange has been thickened with respect to the NU girder, increasing from 65 to 75 mm (2.56 to 2.95 in.). In addition, the slope on the bottom of the top flange has been increased over that of the NU girder series to be more in line with current WSDOT standard girders. Based on experience, both the flange thickening and slope increase were deemed necessary to prevent chronic problems with cracking of the top flange when removing the forms.

### Strand Configuration

For pretensioned girders, the configuration of straight strands and harped strands between the harp points is shown in Fig. 3, and the harped strand pattern at the girder ends is shown in Fig. 5. Due to the size of the girders,

15.24 mm (0.60 in.) diameter strands at 50 mm (1.97 in.) on center must be used to realize the full potential of the sections. The bottom flange can accommodate 46 straight strands. Harped strands are arranged in a maximum of nine strands per bundle at 75 mm (2.95 in.) spacing between the harp points. Harp points are assumed to be at 40 percent of the span length from the centerline of bearing, and the ratio of straight to harped strands is assumed to be approximately 2 to 1.

All calculations in this paper assume the top pair of harped strands exit the girder ends at 50 mm (1.97 in.) from the top of the girder. However, in design, the location where the harped strands exit the girder ends should be held as low as possible while still maintaining the concrete stresses within allowable limits (the center of gravity of all strands at or slightly above the lower kern). This will reduce the demand on the pretensioning abutments.

The exit location of the harped strands is strongly dependent on the handling and shipping schemes neces-

sary to maintain the stability of the girder, as discussed later in this paper. For safety reasons, the slope of the harped strands should not exceed 8 horizontal to 1 vertical. This maximum slope is somewhat arbitrary at this time because strand manufacturers have not been able to provide a maximum safe slope for pretensioned 15.24 mm (0.60 in.) diameter strand.

For post-tensioned girders, the tendon layout at midspan is shown in Fig. 4, and at the anchorage locations in Figs. 7 and 8. Anchorage locations may vary depending on the size of the anchorage. The minimum 25 mm (0.98 in.) clear distance between ducts should be maintained throughout the entire length of the tendon until the individual ducts diverge into the anchorages.

Where necessary, pretensioned strands can be added to supplement the post-tensioning tendons and to carry loads imposed on the girder prior to post-tensioning. Harped pretensioned strands should be avoided unless they can be arranged so as not to interfere with the post-tensioning ducts and anchorages. Concrete stresses at the girder ends at the release of straight pretensioned strands can be controlled by debonding a predetermined number of strands for some distance from the ends.

### End Blocks and Transitions

Figs. 7 and 8 show that four post-tensioning anchor plates up to 406 mm (16.00 in.) square can fit in the end of a W21PTMG girder with the addition of a 500 mm (19.69 in.) wide end block. This is thought to be the largest commercially available anchor plate for the tendon sizes noted previously. "Special" anchorages, as defined by the 1994 AASHTO LRFD Bridge Design Specifications, are smaller than plate anchorages and will easily fit in the same end block. The end block length is 1000 mm (39.37 in.) with a transition length of 1500 mm (59.06 in.).

End blocks and transitions are only required where the post-tensioning anchorages are intended to be embedded in the girder ends. This most frequently applies to girders that are fabricated in one piece and post-tensioned in the producer's yard (in cases where

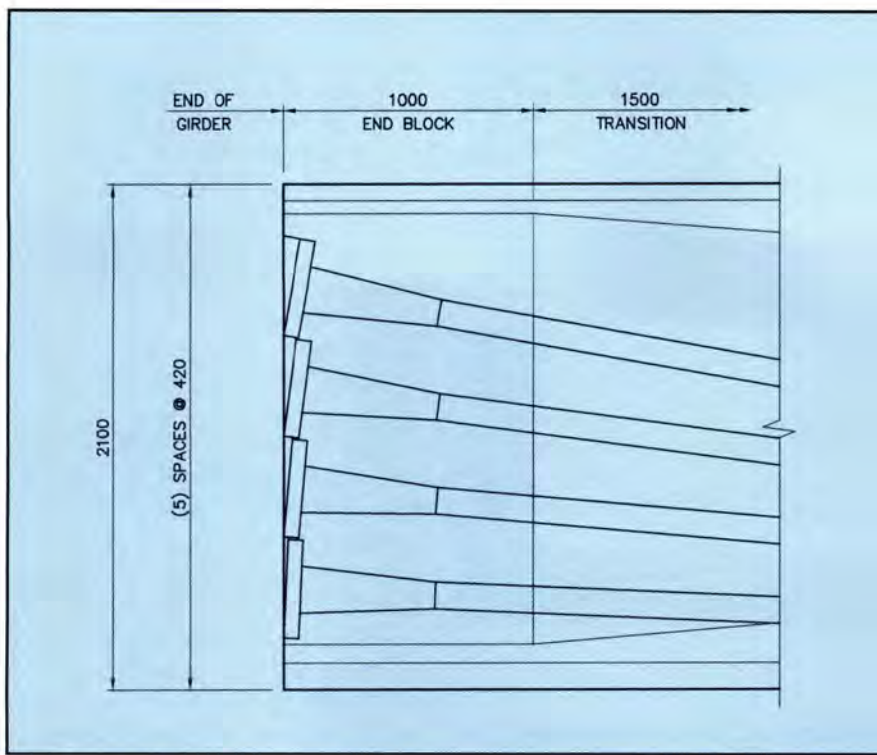


Fig. 8. Post-tensioning anchor layout.

the precasting plant does not have sufficient pretensioning capability) or when girders are assembled and post-tensioned on the ground and erected in one piece. When girders are assembled in place, it is usually most convenient to embed the post-tensioning anchorages in large end diaphragms, which can be easily reinforced to withstand the large concentrated forces generated by the post-tensioning process.

### Girder Efficiency

Two formulas have been proposed for assessing the efficiency of prestressed concrete flexural members. Guyon<sup>6</sup> proposed an equation based on maximizing section moduli for the top and bottom fibers for a given cross-sectional area. This efficiency factor,  $\rho$ , is defined as:

$$\rho = \frac{r^2}{y_t y_b}$$

where

- $r$  = radius of gyration of section =  $\sqrt{I/A_c}$
- $y_t, y_b$  = distance from center of gravity to top and bottom fibers, respectively
- $I$  = moment of inertia
- $A_c$  = cross-sectional area

Aswad<sup>7</sup> proposed an efficiency ratio based on the stress in the bottom fibers. This efficiency ratio,  $\alpha$ , is defined as:

$$\alpha = \frac{3.46 S_b}{A_c h}$$

where

- $S_b$  = section modulus for bottom fibers
- $A_c$  = cross-sectional area
- $h$  = depth of section

Different girder cross sections from across the country have been compared using these formulas.<sup>8</sup> Figs. 9 and 10 show plots of these efficiency factors for various types of girders. As can be seen, the new WSDOT pretensioned girders rank among the highest efficiency factors. When compared to the NU girders, calculations indicate that, depending on which formula is used, the proposed sections are either slightly more or slightly less efficient than their NU counterparts. Because WSDOT does not allow tension in the bottom fibers under service loads, the Aswad efficiency ratio may not be an appropriate indicator of the efficiency of the section for its intended use. A direct comparison of pretensioned span capabilities of the new WSDOT sec-

tions and the NU girder series will be made later in this paper.

## PRETENSIONED SPAN CAPABILITIES

The span capabilities of the new WSDOT pretensioned sections are highly dependent on the assumptions made in the design. The following section presents the design criteria used to develop the baseline span capability envelopes. In general, these are the same criteria used by WSDOT to design prestressed concrete girders. Subsequent sections show the consequences of varying specific design assumptions on span capabilities. All span capabilities are shown in U.S. Customary Units.

### Design Criteria for Pretensioned Girders

The design criteria used to develop the baseline span capability envelopes for pretensioned girders are as follows:

1. 1994 AASHTO LRFD Bridge Design Specifications.
2. Dead Load: Girder + Deck + 50 psf (2.39 kPa) + Concrete Diaphragms at 40 ft (12.19 m) maximum.
3. Vehicular Live Load: AASHTO HL-93, including 33 percent impact on truck portion only.
4. Limit States: Service-I (Compression) and Service-III (Tension), Strength-I.
5. Live Load Distribution: Approximate method for both flexure and shear, interior beams.
6. Girder Spacing: 5 to 10 ft (1.52 to 3.05 m).
7. Concrete:
  - Girder  $f'_c = 10.0$  ksi (68.95 MPa),  $w_c = 156$  pcf (24.51 kN/m<sup>3</sup>)
  - Deck  $f'_c = 6.0$  ksi (41.37 MPa),  $w_c = 155$  pcf (24.35 kN/m<sup>3</sup>)
  - $\gamma_c = 160$  pcf (25.13 kN/m<sup>3</sup>) used in weight calculations
  - $f'_{ci} = 4.0$  ksi (27.58 MPa) minimum
8. Deck Thickness: 7.87 in. (200 mm), unshored, including 0.5 in. (12.70 mm) wearing surface.
9. Prestressing: 0.6 in. (15.24 mm) diameter, 270 ksi (1862 MPa), low-relaxation strand,  $f_{po} = 202.5$  ksi (1396 MPa).

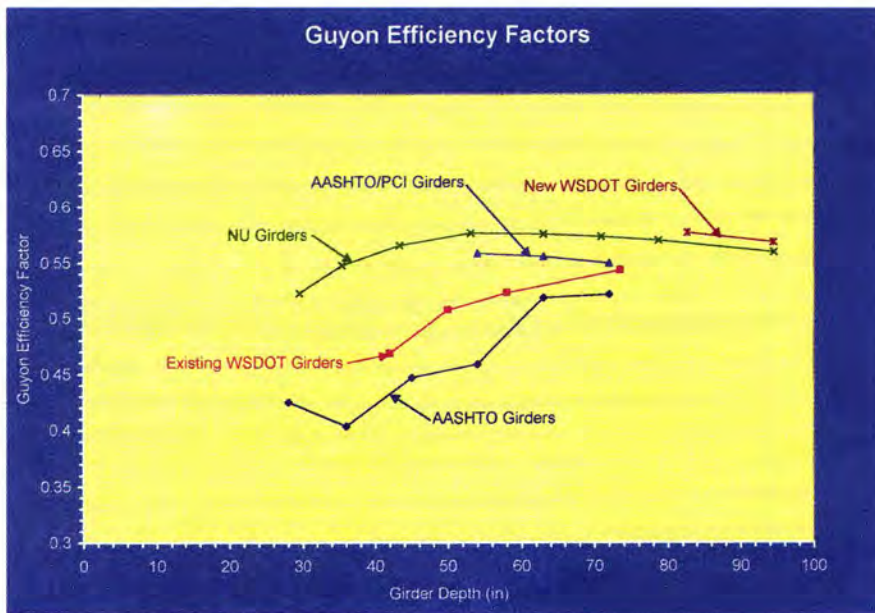


Fig. 9. Guyon efficiency factors (Ref. 6).

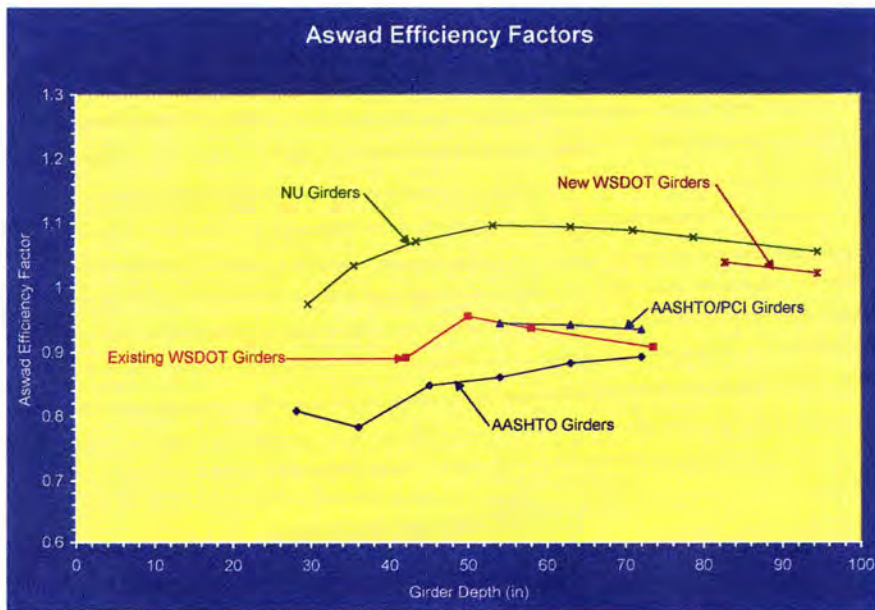


Fig. 10. Aswad efficiency factors (Ref. 7).

**10. Prestress Losses:** AASHTO LRFD Approximate Lump Sum Method or AASHTO LRFD Refined Method, whichever results in less calculated loss.

**11. Allowable Stresses:**

At Service:

Tension = 0

Compression due to permanent loads =  $0.45(f'_c)$

Compression due to all loads =  $0.6(f'_c)$

At Release:

Tension =  $0.22\sqrt{f'_{ci}}$   
( $f'_{ci}$  in ksi)

$$\text{Compression} = 0.6(f'_{ci})$$

A simple span design is assumed for all loads.

**Pretensioned Simple Span Capabilities**

The span capability envelope for the W21MG girder section is shown in Fig. 11. This envelope assumes that the maximum pretensioning capability of precasting plants in the Northwest is sixty-four each 0.6 in. (15.24 mm) diameter strands, and that 200 kips (889.6 kN) is the maximum weight that can be handled and shipped. This

translates into a maximum single-piece girder length of approximately 185 ft (56.39 m). Subsequent sections will examine the influence of varying design assumptions on this envelope.

The span capability envelope of the W24MG girder section is shown in Fig. 12. The maximum single-piece girder length is approximately 172 ft (52.42 m). The influence of varying design assumptions on this envelope will be similar to that of the W21MG girder.

Fig. 11 contains a dotted line labeled "over-reinforced." For sections to the right of this line, the ratio of the depth of the neutral axis to the moment arm of the prestressed reinforcement exceeds the limit of 0.42 (AASHTO LRFD Section 5.7.3.3.1). For these cases, the equation given for the maximum nominal flexural resistance of over-reinforced sections (AASHTO LRFD Section C5.7.3.3.1) is used. Over-reinforced sections do not occur in the pretensioned range of the W24MG girder. Further discussion of over-reinforced sections will be provided later in this paper.

**Prestress Losses**

One of the most significant variables influencing the span capability of prestressed concrete girders is the method used to calculate long-term prestress losses. Fig. 13 plots calculated prestress losses for W21MG girders at a 10 ft (3.05 m) spacing using four different methods. The PCI General Method<sup>9,10</sup> is a time-step calculation that considers the interaction of the different components of loss during successive intervals of time. The other three methods result in lump sum values for the final prestress loss. For this particular girder configuration, the AASHTO LRFD Refined Method results in the greatest calculated loss, while the method recommended by ACI-ASCE Committee 423<sup>11</sup> results in the least.

The influence of calculated long-term prestress losses on the span capability envelope of a W21MG girder is shown in Fig. 14. For the entire range, the loss of span capability from one extreme to the other is 5 to 13 percent. At higher levels of pretensioning, the available span can be reduced by more

than 18 ft (5.49 m). This will undoubtedly be accentuated with the longer-span post-tensioned girders.

Pessiki et al.<sup>12</sup> have recently evaluated the effective prestress force in two 28-year-old prestressed concrete bridge beams. Their conclusion was that the average actual loss experienced by these beams was approximately 60 percent of the losses predicted using current calculation methods. Similar results have been reported over the past decade.<sup>13,14</sup>

The beam section studied by Pessiki et al. is shown in Fig. 15, along with material and section properties. Some properties were measured and recorded in the study, while others were assumed for the sake of calculation. Prestress loss values calculated by the four methods described above, as compared to the measured losses, are shown in Table 1.

All predicted values overestimate the actual losses, with the ACI-ASCE Committee 423 Method providing the closest estimate. For the purpose of this paper, subsequent sections will use either the AASHTO LRFD Approximate or Refined Methods, whichever results in the lesser value. However, significant benefits can be derived from using a more rigorous method for calculating prestress losses. WSDOT has developed their own time-step, rate-of-creep method, which is used to evaluate prestress losses in prestressed concrete girders outside of the usual design range.

### Design Specification

Fig. 16 compares the span capability envelopes for the W21MG girder section using both the 1994 AASHTO LRFD Bridge Design Specifications and the 1996 AASHTO Standard Specifications for Highway Bridges, 16th Edition.<sup>15</sup> To ensure a consistent comparison of the design specifications, minimum prestress losses as calculated by the AASHTO LRFD Approximate or Refined Methods are used for both envelopes. The difference between the two envelopes is nominal, indicating that the choice of design specification has little impact on the span capabilities of the girder sections.

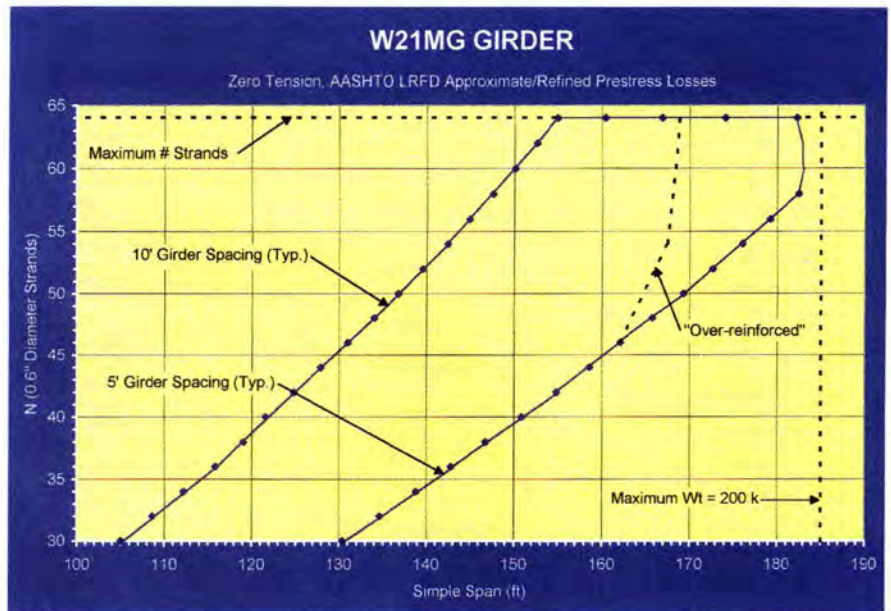


Fig. 11. W21MG span capability envelope.

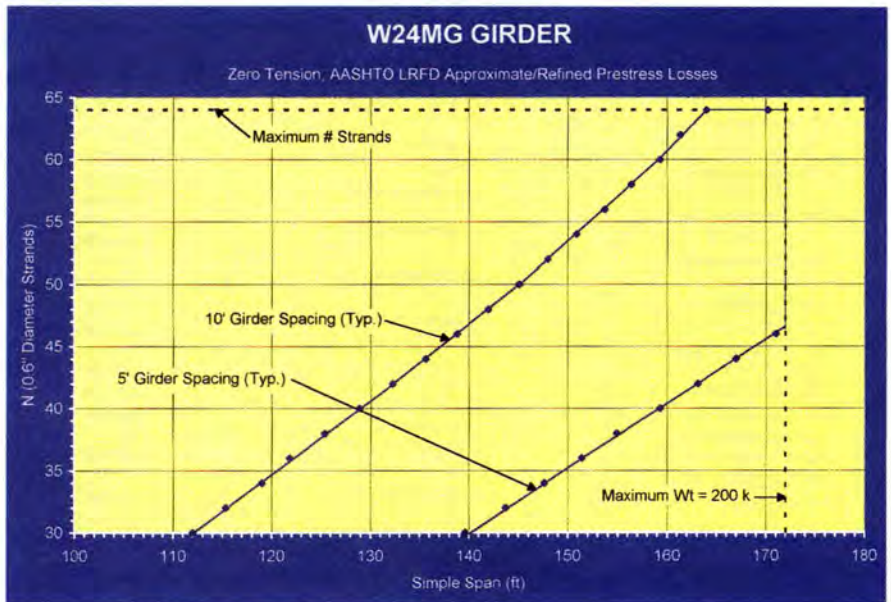


Fig. 12. W24MG span capability envelope.

### Allowable Tension

Another significant variable influencing span capability is the amount of tension allowed in the precompressed tensile zone at the service limit state. The 1994 AASHTO LRFD Bridge Design Specifications allow  $0.19\sqrt{f'_c}$  (formerly  $6\sqrt{f'_c}$  for  $f'_c$  in psi) tension for all components not subjected to severe corrosive conditions. Tension in components subjected to severe corrosive conditions is limited to  $0.0948\sqrt{f'_c}$  (formerly  $3\sqrt{f'_c}$  for  $f'_c$  in psi). Currently, WSDOT allows no

tension in the precompressed tensile zone under service loads.

Fig. 17 shows the impact on span capabilities of the W21MG girder section for the three levels of allowable tension noted above. There are several ways to interpret this chart. On the vertical axis, each interval of allowable tension represents a savings of between four and five strands for the same span and girder spacing, along with the concurrent reduction in required concrete release strength. This is probably the least consequential interpretation.



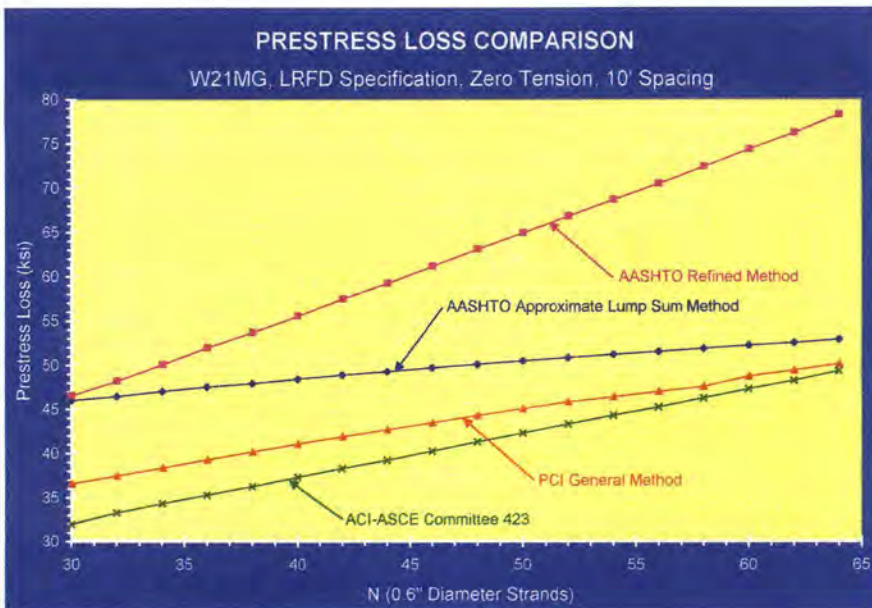


Fig. 13. Prestress loss comparison.

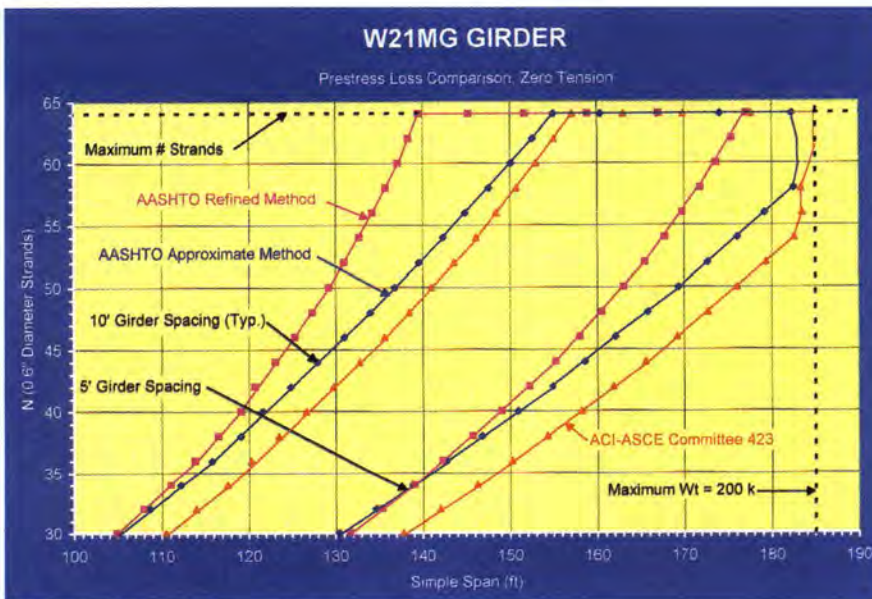


Fig. 14. Prestress loss envelope comparison.

On the horizontal axis, each allowable tension interval represents an increase in span capability of between 5 and 10 ft (1.52 and 3.05 m) for the same number of strands and girder spacing. The most significant interpretation is that for each allowable tension interval, the same girder section can be spaced roughly 1 ft (0.30 m) further apart. This can lead to considerable savings if one or more lines of girders can be eliminated.

### Deck Thickness

As previously mentioned, the baseline span capability envelopes were de-

rived assuming a 6.0 ksi (41.37 MPa), 7.87 in. (200 mm) thick deck with a 0.5 in. (13 mm) wearing surface. Fig. 18 compares this baseline envelope with envelopes for 8.86 and 9.84 in. (225 and 250 mm) thick decks, all at strengths of 6.0 ksi (41.37 MPa). Deck thickness is typically a function of girder spacing rather than girder depth. The increased weight of the thicker deck predictably reduces the available span, though not by a large amount. The increased deck thickness also increases the available span range before the members become over-reinforced.

WSDOT has selected a standard deck thickness of 8.86 in. (225 mm) with a 0.39 in. (10 mm) wearing surface for use with the new deep girder sections.

### Deck Strength

Fig. 19 compares envelopes for an 8.86 in. (225 mm) thick deck at strengths of 4.0, 5.0, 6.0, and 8.0 ksi (27.58, 34.48, 41.37, and 55.16 MPa). Within the envelope range where allowable stresses govern the design, the increased deck strength marginally increases the available span range. However, deck strength has a significant impact on the point at which the sections become over-reinforced, as well as the point at which the flexural strength becomes inadequate. A deck strength of 8.0 ksi (55.16 MPa) eliminates over-reinforced sections from the available span range. A deck strength of 6.0 ksi (41.37 MPa) provides adequate flexural strength throughout the range. In general, it appears to be more efficient to increase the strength of the deck instead of its thickness, although stronger decks can pose other problems, such as obtaining a satisfactory finish on the wearing surface.

WSDOT currently specifies a standard deck strength of 4.0 ksi (27.58 MPa). It may be necessary to increase this strength in the upper reaches of the pretensioned span range to ensure adequate flexural strength. However, a few design criteria modifications can be used to help alleviate this problem. First, typical design practice conservatively neglects the area of the top flange of the girder when calculating the depth to the neutral axis. For these sections, the top flange provides a relatively large area of high strength concrete, which effectively reduces the depth to the neutral axis.

Also, WSDOT currently designs all girders as simple spans, though they are made continuous for dead loads applied subsequent to the deck pour, and all live loads, with mild steel reinforcement in the deck over the piers. Some reduction in midspan positive moments due to continuity would help reduce the demand on the deck.

Finally, a more rigorous analysis procedure, such as strain compatibil-

ity, can be employed to determine the flexural resistance of the member. Section 8.2.2.5 of the PCI Bridge Design Manual<sup>16</sup> provides a rational approach to strength calculations.

### Comparison with the Pretensioned NU Girder Series

Fig. 20 plots the span capability envelopes of the W24MG and the NU2400 girder sections. These envelopes are virtually identical, with the exception of the maximum single-piece girder length. Because the W24MG section is slightly heavier than the NU2400, its length is limited to 172 ft (52.42 m) vs. 180 ft (54.86 m) for the NU2400.

There is no direct counterpart for the W21MG girder section in the NU series, so no comparison of span capability was made.

### Concrete Strengths

The required concrete release strengths are shown in Fig. 21 for different span and strand configurations. These strengths were calculated assuming the lifting devices are located to ensure a minimum level of stability during stripping without additional bracing. The required strengths range from a minimum of 4.0 ksi (27.58 MPa) to a maximum of over 8.0 ksi (55.16 MPa). Overnight strengths of up to 7.2 ksi (49.64 MPa) have been consistently attained at Concrete Technology Corporation (CTC) with concrete mixes containing silica fume. Higher release strengths can be achieved on an every-other-day basis with added cost.

As mentioned previously, the design concrete strength used to develop the span capability envelopes was 10.0 ksi (68.95 MPa). This value is the maximum that PNW/PCI members feel they can consistently achieve at this time. However, it should be emphasized that specific projects will not usually require design strengths of this magnitude. Based on flexure only, if the span capability envelope of Fig. 11 were replotted for 6.0 ksi (41.37 MPa) concrete in the girder, the span capability is reduced by less than 0.5 percent. Of course, this limits the range of available span and spacing configurations to those below the line labeled

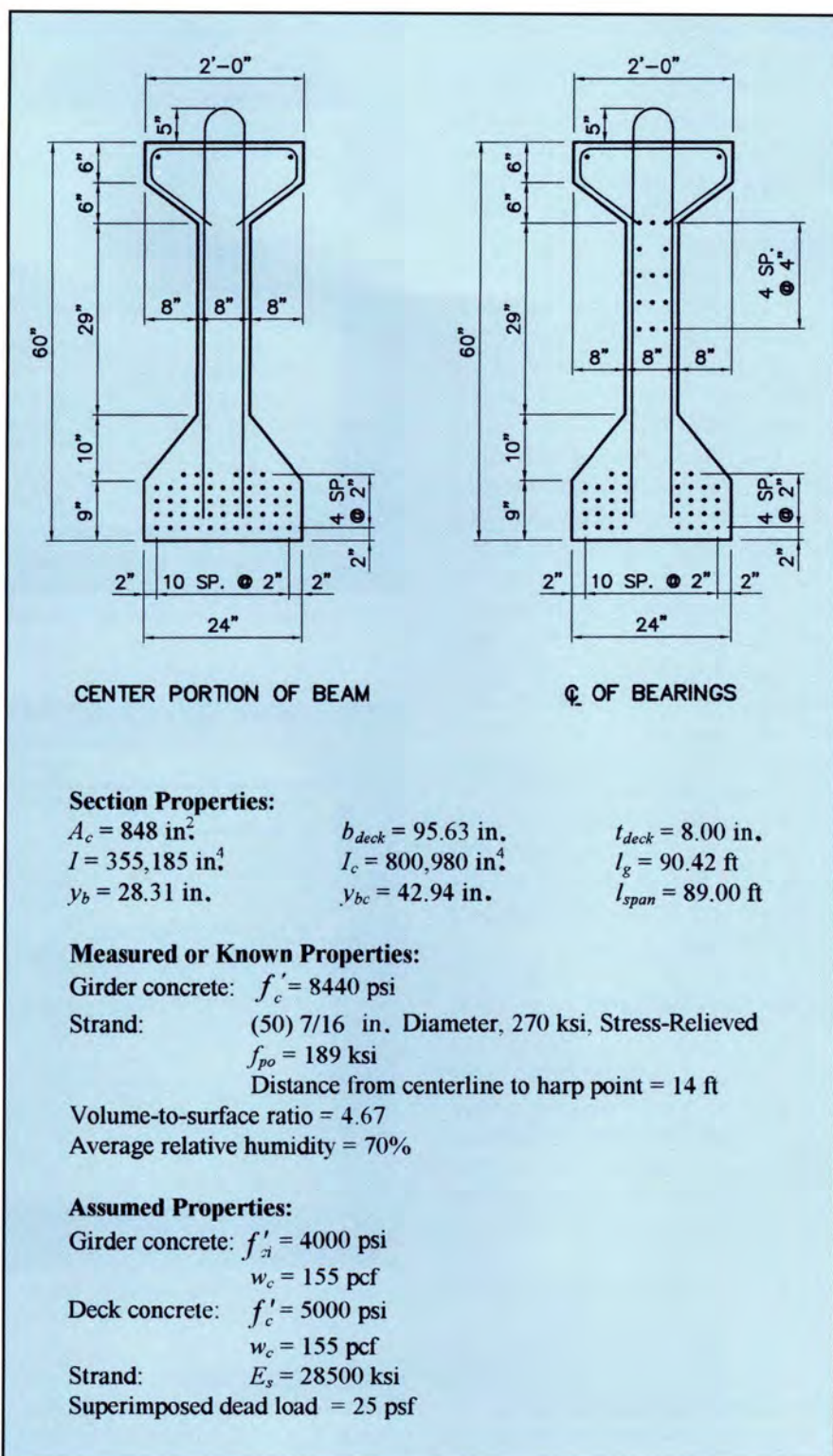


Fig. 15. Beams studied by Pessiki et al. (Ref. 12).

Table 1. Calculated prestress losses for beams studied by Pessiki et al. (Ref. 12).

Method	ES (ksi)	SR (ksi)	CR (ksi)	REL (ksi)	Total (ksi)
AASHTO Refined	13.56	6.50	17.47	16.27	53.80
AASHTO Approximate	13.56	—	—	—	50.55
PCI General	10.84	8.56	9.19	18.65	47.24
ACI-ASCE Committee 423	13.15	5.05	10.74	15.66	44.60
Average measured losses	—	—	—	—	34

$f'_{ci} = 6000$  psi (41.37 MPa) in Fig. 21.

The applied criteria of zero tension and simple spans results in the concrete strength at release governing the design. Zero tension is zero tension, whether it is applied to 10.0 ksi (68.95 MPa) concrete or 6.0 ksi (41.37 MPa) concrete. Simple spans place the demand for compression resistance in the cast-in-place deck, rather than in the girder. This would not be the case for girders made continuous, or for girders in which tension is allowed at the service limit state.

Additionally, industry statistics have shown a strong correlation between concrete release strength, curing time and temperature, and the design concrete strength. For a given mix design, the more aggressively the concrete is cured to achieve a high release strength, the lower the long-term strength will be. Consequently, it is recommended that both the release and design concrete strengths be specified as the minimum required by design for the specific project, rounded up to the nearest 0.10 ksi (0.69 MPa), but not less than 4.0 ksi (27.58 MPa) at release and 7.0 ksi (48.27 MPa) at 28 (or 56) days.

### Section Finalization

In the interest of finalizing the new WSDOT sections, PNW/PCI and WSDOT separately retained the services of BERGER/ABAM Engineers (B/A), Inc., Federal Way, Washington, to provide final detailed engineering and drafting of the Standard Plans for pretensioned sections only. PNW/PCI assumed responsibility for providing engineering calculations and sketches, while WSDOT provided funding for drafting. The scope of the work B/A performed included the following:

1. For sections between the end of the girder and  $d_v$ , size the required web reinforcement to resist the worst-case bursting and splitting forces.

2. For sections  $d_v$  from the center of bearing and beyond, evaluate the required web reinforcement for shear based on the AASHTO LRFD Specifications.

3. Evaluate the maximum required bearing pad size and distance from the end, and modify the standard details accordingly.



Fig. 16. Design specification comparison.



Fig. 17. Allowable tension comparison.

4. For girder ends that tie directly into piers or hinges through shear friction, evaluate the size and distance from the girder end to the temporary oak blocks that support the girders during construction. Also, evaluate the quantity of shear friction reinforcement projecting from the end of the girder.

5. Size and detail high strength lifting bars for girders weighing more than the capacity of standard lift loops.

6. Provide sample calculations for evaluating the stability of the girders during lifting.

7. Size the worst-case intermediate cast-in-place concrete diaphragm, and modify the standard details accordingly.

Performance of this scope of work resulted in the generation or modification of 28 Standard Plan sheets, half of which were in U.S. Customary Units, the other half in S.I. Units. Appendix C contains the Standard Plans for the W21MG section. These plans have been stamped "Preliminary" because they had not yet been finalized at the time they were submitted for this paper.

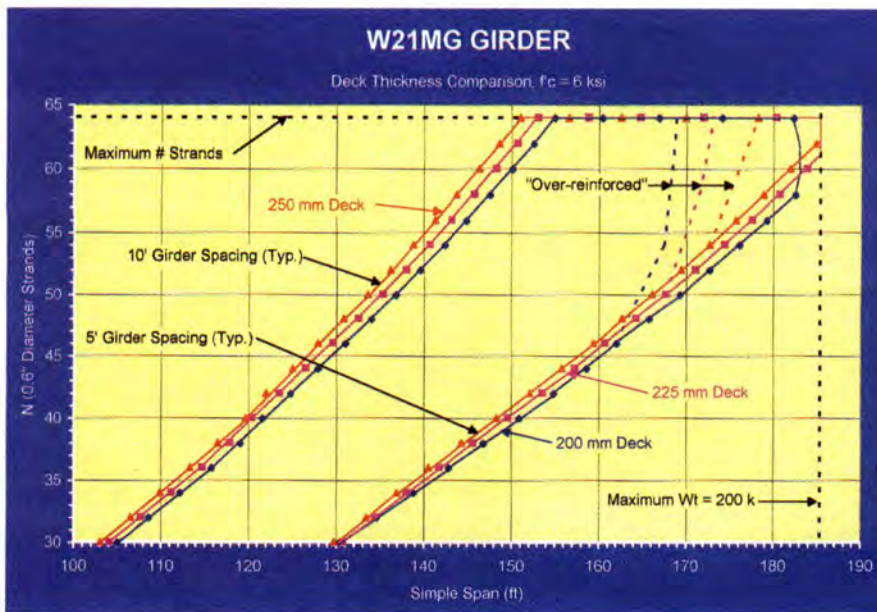


Fig. 18. Deck thickness comparison.

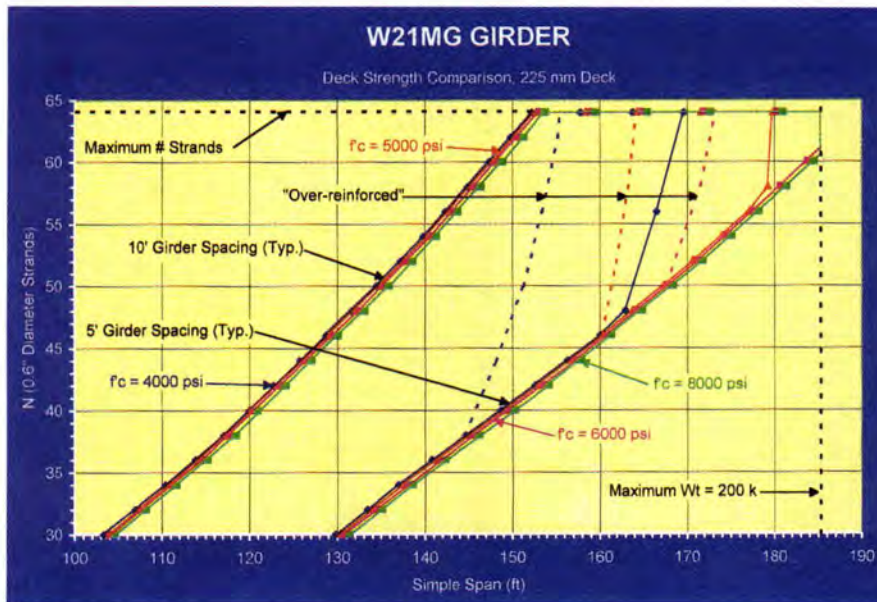


Fig. 19. Deck strength comparison.

### Web Reinforcement

A standardized stirrup spacing was established for the end of the girder by hand calculations using the Hal Birkland Beam Method. A finite element model was used to confirm the results of the hand calculation. Though the finite element model indicated that the hand calculations were quite conservative, the results of the hand calculations were used to size the web reinforcement. The resulting configuration is very similar to that used on existing WSDOT standard girders.

For shear beyond the standard end configuration, calculations indicate that pairs of #4 stirrups at 18 in. (460 mm) on center should be sufficient for most design cases.

### Primary Uses of Pretensioned Deep Girder Sections

As discussed previously, one of the primary uses of the new pretensioned WSDOT girder sections is to increase the span capabilities of standard prestressed concrete girders. Assuming zero tension, the W21MG section can span up to 182 ft (55.47 m) at a 6 ft

(1.83 m) girder spacing. Allowing some tension at the service limit state can increase the girder spacing, or reduce the required number of strands. The current standard W74MG section can span up to 160 ft (48.77 m) at a 4 ft (1.22 m) girder spacing. Due to weight considerations, the length of the W24MG section is limited to 172 ft (52.42 m). Consequently, the primary section for extending pretensioned girder spans is the W21MG.

The second primary use of the new WSDOT girder sections is to improve economy by increasing the girder spacing over designs using existing standard girders. As discussed above, the W74MG can span up to 160 ft (48.77 m) at a 4 ft (1.22 m) girder spacing. The same span can be achieved with a W21MG girder at a 9 ft (2.74 m) spacing, or a W24MG girder at nearly 11 ft (3.35 m). The number of girder lines required per span can be significantly reduced for bridges that can tolerate the additional superstructure depth.

## HANDLING AND SHIPPING OF DEEP GIRDER SECTIONS

Considerations for handling and shipping deep girder sections relate primarily to weight, length, height and lateral stability. The effect of each variable differs considerably depending on where the handling is taking place: in the plant, on the road, or at the jobsite.

### In-Plant Handling of Deep Girder Sections

The primary considerations for in-plant handling are weight and lateral stability. As previously mentioned, the maximum weight that can be handled by precasting plants in the Pacific Northwest is 200 kips (889.6 kN). Pretensioning lines are normally long enough so that the weight of a girder governs capacity, rather than its length. Headroom is also not generally a concern for the deeper sections.

Lateral stability can be a concern when handling long, slender girders. When the girder is stripped from the form, the prestressing level is higher and the concrete strength is lower than at any other point in the life of the

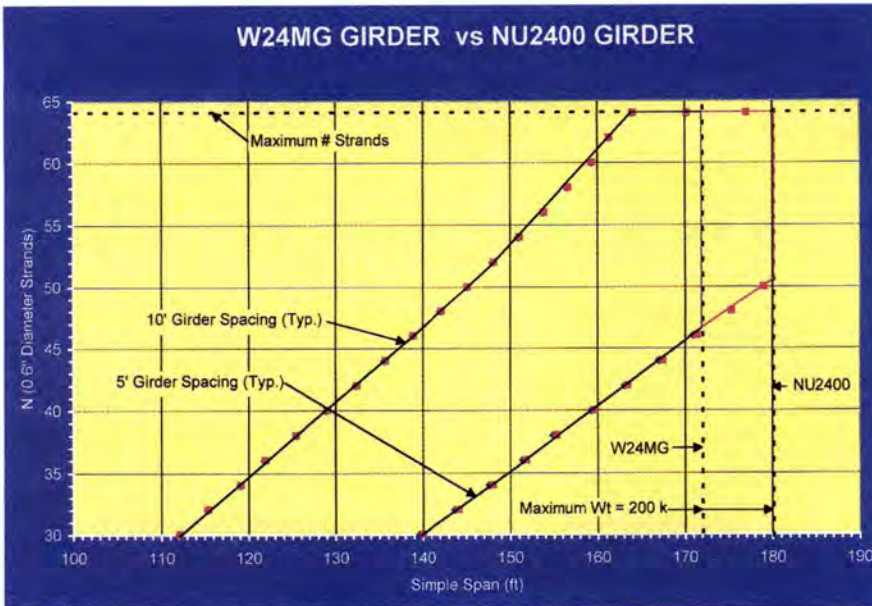


Fig. 20. Comparison of span capabilities — W24MG vs. NU2400.



Fig. 21. W21MG girder handling without bracing.

member. Mast<sup>17,18</sup> has developed methods for evaluating the lateral stability of long slender members during lifting. Imper and Laszlo<sup>19</sup> describe methods for bracing long slender girders for improved stability.

The new girder sections are relatively wide and stiff about their weak axes and, as a result, exhibit good stability, even at their longer pretensioned lengths. As noted by Mast, the simplest method of improving stability is to move the lifting devices away from the ends. This invariably increases the required concrete release

strength, because decreasing the distance between lifting devices increases the concrete stresses at the harp point. Stresses at the support may also govern, depending on the exit location of the harped strands.

Fig. 21 shows lifting device locations and resulting concrete release strengths that provide the minimum recommended stability for a W21MG girder without additional bracing, assuming the top harped strands exit at 50 mm (1.97 in.) from the top of the girder. This envelope has been expanded to include tension in the con-

crete at service up to the maximum allowed by the 1994 AASHTO LRFD Bridge Design Specifications.

Alternatively, the new girder sections may be braced to provide adequate stability. Imper and Laszlo discuss adding temporary prestressing to the top flange to provide a larger factor of safety against cracking. Cracking of the top flange degrades the lateral stiffness of the section, and in turn reduces its lateral stability.

Fig. 22 shows the effects of adding four temporary 0.6 in. (15.24 mm) diameter strands, jacked to the same level as the permanent strands, to the top flange. If the temporary prestress is introduced prior to stripping the girder from the form, the lifting devices may be placed closer to the ends while still maintaining adequate stability. This, in addition to the temporary reduction of the eccentricity of the total prestress force, reduces the concrete stresses and allows a reduction in the required release strength.

Other types of bracing have also been used successfully for many years. These systems are generally based on experience rather than theory. Other methods of improving lateral stability, such as raising the roll axis of the girder,<sup>19</sup> are also available. Sample calculations for handling the new WSDOT girder sections are provided in Appendix D.

### Shipping of Deep Girder Sections

The ability to ship deep girder sections can be influenced by a large number of variables, including mode of transportation, weight, length, height and lateral stability. Some variables are more restrictive than others. As such, the feasibility of shipping deep girders is strongly site-dependent. The author recommends that routes to the site be investigated during the preliminary design phase. To this end, on projects using long, heavy girders, WSDOT will place an advisory in their Special Provisions including shipping routes, estimated permit fees, escort vehicle requirements, Washington State Patrol requirements, and permit approval time.

## Mode of Transportation

Three modes of transportation are commonly used in the industry: truck, rail and barge. In Washington State, an overwhelming percentage of girders is shipped by truck, so discussion in subsequent sections will be confined to this mode. However, on specific projects, it may be economical to consider rail or barge transportation.

Standard rail cars can usually accommodate larger loads than a standard truck. Rail cars range in capacity from approximately 120 to 200 kips (533.8 to 889.6 kN). However, unless the rail system runs directly from the precasting plant to the jobsite, members must be trucked for at least some of the route, and weight may be restricted by the trucking limitations.

Dimensionally, delivery by rail can be significantly more restrictive than by truck. Rail tunnel and other clearances are generally minimized for standard cars, and are often very tight. Long precast members may span several rail cars, and require at least one end support to articulate to accommodate the relative turning radius of each car, which can exacerbate horizontal clearances at the midpoint of the member. Dimensional limitations for rail delivery are heavily route dependent, and must be tightly coordinated with the railroad. Relative to trucks, rail cars are difficult to obtain on a consistent and reliable basis.

For marine construction, barge transportation is usually most economical. Product weights and dimensions are generally not limited by barge delivery, but by the handling equipment on either end. In most cases, if a product can be made and handled in the plant, it can be shipped by barge. Of course, this applies only if both the plant and jobsite are fully accessible by barge.

## Weight Limitations

Girders shipped in some states have weighed in excess of 200 kips (889.6 kN). The net weight limitation with trucking equipment currently available in Washington State is approximately 167 to 180 kips (742.9 to 800.7 kN), if a reasonable delivery rate (number of pieces per day) is to be maintained.

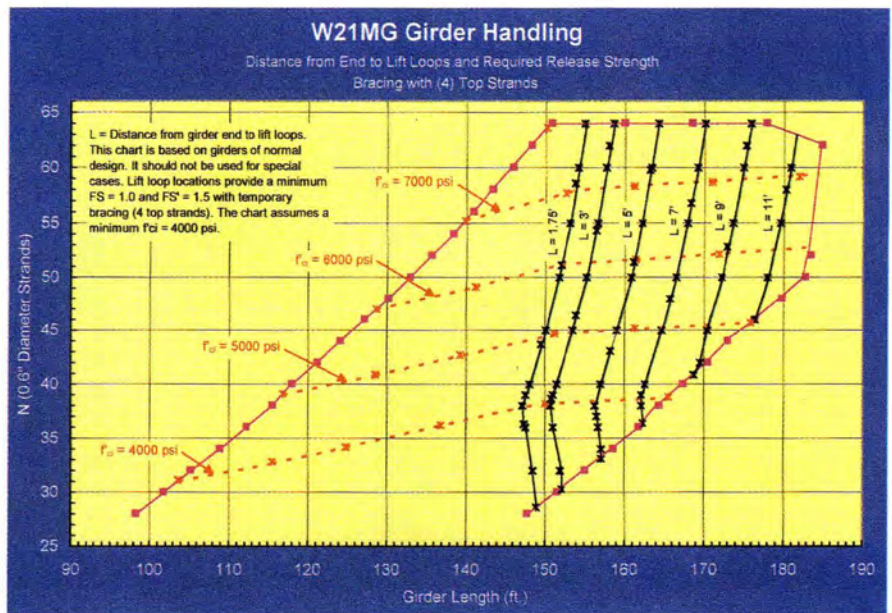


Fig. 22. W21MG girder handling with four temporary top strands.

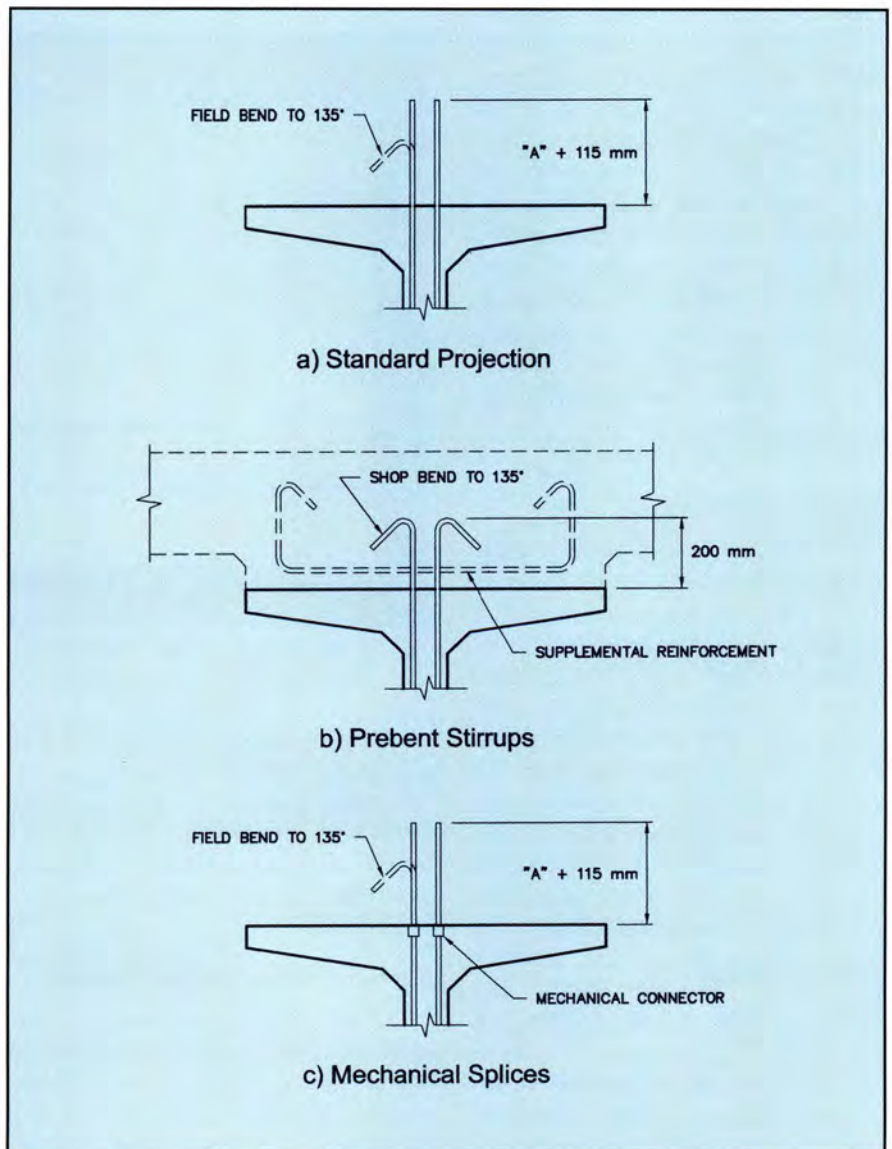


Fig. 23. Alternate stirrup projections.

Product weights of up to 200 kips (889.6 kN) can be hauled with currently available equipment at a limited rate. This can be upgraded to a reasonable rate by round-tripping the equipment if the jobsite is in close proximity to the plant, or to a rail siding or barge unloading facility.

Local carriers should be consulted on the feasibility of shipping heavy girders on specific projects. Of course, girders can be fabricated and shipped in two or more segments to reduce the weight. However, it is more economical to fabricate and ship a single-piece pretensioned girder whenever possible.

### Length Limitations

Length limitations are generally governed by turning radii on the route to the jobsite. Potential problems can be circumvented by moving the support points closer together (away from the ends of the girder), or by selecting alternate routes. A rule of thumb of 130 ft (39.62 m) between supports is commonly used. The sample calculations of Appendix D indicate that, on long pretensioned deep girders, the support points can be moved substantially away from the ends while still maintaining the concrete stresses within allowable limits. Length limitations are not expected to be the governing factor for most project locations.

### Height Limitations

The height of a deep girder section sitting on a jeep and steerable trailer is of concern when considering overhead obstructions on the route to the jobsite. The height of the support is approximately 6 ft (1.83 m) above the roadway surface. When adding the depth of the girder, including camber, the overall height from the roadway surface to the top of concrete can rapidly approach 14 ft (4.27 m). Overhead obstructions along the route should be investigated for adequate clearance in the preliminary design phase. Obstructions without adequate clearance can be bypassed by selecting alternate routes.

Expectations are that, in some cases, overhead clearance will not accommodate the vertical stirrup projection common on shallower WSDOT stan-

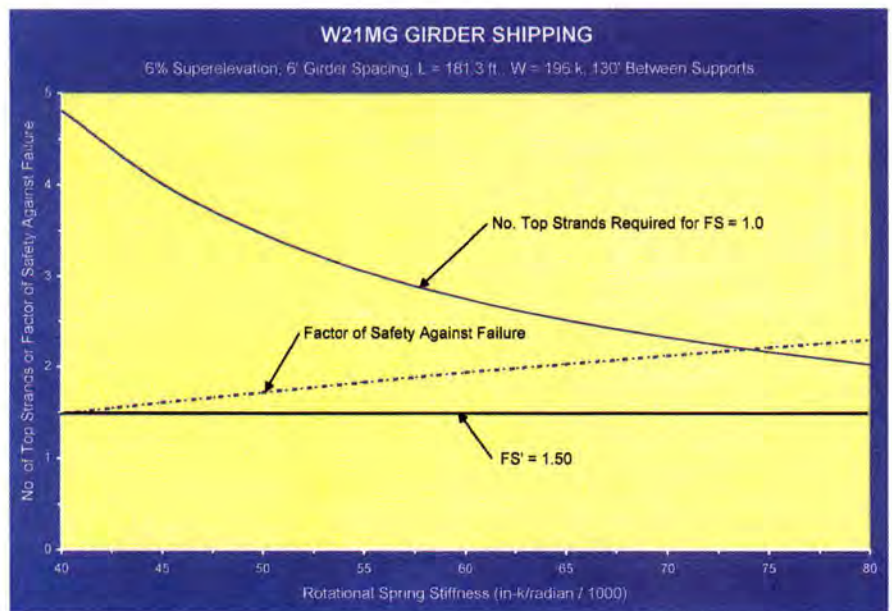


Fig. 24. W21MG factors of safety during shipping.

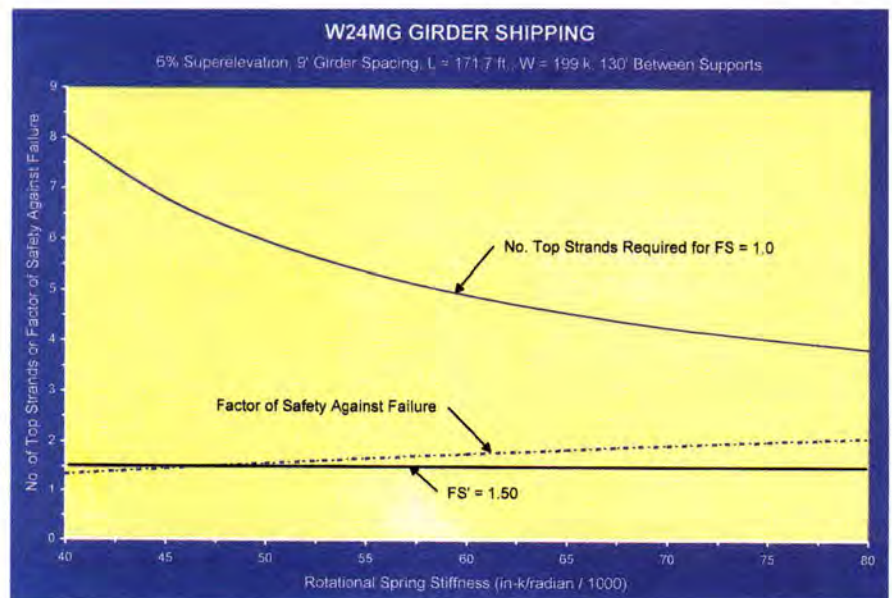


Fig. 25. W24MG factors of safety during shipping.

ard girder sections, as shown in Fig. 23a. Alternate stirrup configurations, as shown in Figs. 23b and c, can be used interchangeably to attain adequate clearance, depending on the route from the plant to the jobsite.

### Lateral Stability During Shipping

As discussed previously, long, slender members can become unstable when supported near the ends. However, studies by Mast<sup>18</sup> conclude that the stability of girders sitting on flexible supports is governed by the rota-

tional stiffness of the support rather than the girder. Methods used to improve lateral stiffness, as discussed by Imper and Laszlo,<sup>19</sup> do little to prevent the truck from rolling. Tentatively, Mast suggests factors of safety of 1.0 against cracking, and 1.5 against failure (rollover of the truck). However, many girders have been successfully shipped in Washington State with a factor of safety against cracking of less than 1.0. This supports Mast's conclusion that the rotational stiffness of the truck dominates the behavior of the transportation system.

Figs. 24 and 25 show the effects of the truck's rotational spring stiffness on the stability of the new sections at a 6 percent superelevation. These charts represent the longest pretensioned lengths of the W21MG and W24MG girders, respectively. They are considered to be worst-case scenarios for shipping the new sections, either in one piece or segmental sections. A sample calculation for stability during shipping is given in Appendix D.

The control against cracking the top flange is represented by the number of temporary top strands, jacked to the same load as the permanent strands, required to provide a factor of safety of 1.0. This variable depends on the combination of girder dead load, prestressing, and tension in the top flange induced by the girder tilt. The calculated tilt includes both the superelevation and its magnification based on the truck's rotational stiffness.

The factor of safety against rollover is represented by the dotted lines. Measurements taken at CTC indicate that the rotational stiffness of a truck configured to carry a 168 ft (51.20 m) long, 180 kip (800.7 kN) decked bulb tee was approximately 40,000 in.-kips per radian (4519 kN-m/radian). Fig. 26 shows the truck configuration while Fig. 27 shows the measurements being taken. For the W21MG girder, this stiffness would provide a minimum factor of safety of 1.5 for the entire range of span capabilities at up to a 6 percent superelevation.

In contrast, due to the large top flange of the decked bulb tee, calculations indicated a factor of safety of 1.37 at a superelevation of 6 percent. This result is similar to a long W24MG girder, which would have a factor of safety of 1.35 at a 6 percent superelevation. The W24MG girder would require a truck rotational stiffness of approximately 47,000 in.-kips per radian (5310 kN-m/radian) to achieve a factor of safety of 1.5 at a 6 percent superelevation. In any case, the decked bulb tees of Fig. 26 were successfully shipped to a remote location.

With respect to the truck's rotational stiffness, Mast postulates that air suspension provides little or no rotational stiffness. CTC's measurements support this notion. The tractor and trailer



Fig. 26. 168 ft (51.2 m) long, 180,000 lb (81648 kg) decked bulb-tee girder.



Fig. 27. Tractor rotational stiffness measurements.



configurations of the truck shown in Fig. 26 were very similar, except that the tractor had two of its dual axles supported by air suspension. The lateral stiffness of the tractor was measured to be about two-thirds of the trailer. The 40,000 in.-kips per radian (4519 kN-m/radian) value is the sum of the tractor and trailer.

### Erection of Deep Girder Sections

A variety of methods are used to erect precast concrete girders, depending on the weight, length, available crane capacity, and site access. The PCI Bridge Design Manual<sup>16</sup> describes many of these erection scenarios.

As mentioned previously, lifting long girders during erection is not as critical as when they are stripped from the forms, particularly when the same lifting devices are used for both. However, if a separate set of erection devices are used, the girder should be checked for stresses and lateral stability. In addition, once the girder is set in place, the free span between supports is usually increased significantly. Mast<sup>18</sup> points out that this can lead to stability problems, particularly if the supports are "springy." Wind can also pose a problem. Consequently, when long girders are erected, they should immediately be braced at the ends.

### CURRENT PROJECTS

The first application of the new WSDOT deep girder sections is, oddly enough, not in Washington State. The 2002 Olympic Winter Games, to be held in Salt Lake City, has spurred the expansion of Interstate 15, resulting in a \$1.6 billion project including 81 prestressed concrete I-girder bridges. This project is so large that Sverdrup/DeLeuw, the lead joint venture consultant, was given the flexibility to choose any standard girder series that proved to be the most efficient.

For 16 long span bridges, Sverdrup/DeLeuw chose the segmental W24PTMG section, with spans of up to 227 ft (69.19 m). Also incorporated into the project are 65 bridges with shallower versions of the new pretensioned sections. Girder depths were chosen as 1050, 1450 and 1850 mm (41.34, 57.09 and 72.83 in.) to approx-

imate the depths of previously available WSDOT sections.

The first deep girder project in Washington State was designed by BERGER/ABAM Engineers, Inc. for the City of Kent. A modified version of the segmental W21PTMG girder was specified for continuous spans of 120, 183, and 154 ft (36.57, 55.78, and 46.94 m). The bridge geometry is complex, incorporating a horizontal curve, superelevation, and an 8.9 percent grade.

The girder segments consist of nominal 60 ft (18.29 m) long pier head sections with single-piece drop-in segments to fill out all three spans. All segments are chorded to follow the horizontal curve. Modifications to the sections include deepening of the bottom flange over the intermediate piers and an increase in web thickness at all supports. The deepening of the bottom flange was necessary to control stresses due to negative moments and to accommodate a level bearing surface in spite of the severe grade. The widening of the web was necessary for additional shear capacity.

It should be noted that the AASHTO Guide Specifications for Design and Construction of Segmental Concrete Bridges<sup>20</sup> were used in the design of this bridge. It is not certain that the web widening would have been necessary had either the 1994 AASHTO LRFD Bridge Design Specifications<sup>7</sup> or the 1996 AASHTO Standard Specifications for Highway Bridges, 16th Edition<sup>15</sup> been used.

WSDOT is currently in the process of designing their first two bridges using the new girder sections. The Methow Bridge was originally planned as a three-span, W74MG girder superstructure. It now has two spans with pretensioned, single-piece W21MG girders, roughly 177 ft (54 m) long and weighing 192 kips (854.1 kN). This has allowed a pier to be pulled from the water.

The Twisp Bridge was initially envisioned as a two-span W74MG girder bridge. It now has a single 196 ft (60 m) span using the segmental W24PTMG section, which eliminates the water pier entirely. These girders will be assembled in three pieces and post-tensioned together. The contract

will allow the use of temporary support towers to assemble the girders in place or the girders can be assembled in a staging area and subsequently be launched across the river. WSDOT considers the elimination of water piers to be a significant benefit, both from maintenance and environmental perspectives.

Several other bridges using the new girder sections are currently in design for various cities and counties within Washington State.

### CONCLUDING REMARKS

The relationship developed between WSDOT and PNW/PCI has been beneficial to both parties, as well as the regional taxpayers. Mutual cooperation has improved the quality and economy of existing precast, prestressed concrete bridge products. The development of new standard deep girder sections gives WSDOT the ability to extend spans and remove piers from environmentally sensitive areas, all with the superstructure material they prefer to specify. It also gives the producer members of PNW/PCI access to markets that have previously belonged to steel or cast-in-place concrete construction.

PNW/PCI is continuing to work with WSDOT to develop new standards for transportation-related structures and to improve existing standards. Standard details and span capabilities for segmentally constructed I-girder bridges using the newly developed sections are next on the list. Standardizing sections and details for pretensioned or post-tensioned, segmental "tub" girders is also a priority. New sound wall, stay-in-place deck panel, and substructure element standards have also been discussed.

### ACKNOWLEDGMENTS

The author would like to acknowledge the many people who contributed to the development of the deep girder standards. Special thanks go to Myint Lwin, Chuck Ruth, Yum Man Tam, and many others at WSDOT's Bridge and Structures Office. Their enthusiasm and open-mindedness made the development of

the new sections possible. Jerry Weigel of WSDOT's Construction Division provided jobsite construction and contract administration expertise. From WSDOT's Motor Carrier Services, Barry Diseth helped to establish the criteria for shipping these long, heavy girders.

Special thanks are also extended to Dr. Maher Tadros and his colleagues at the University of Nebraska for their work in developing the NU girder se-

ries. Dr. Tadros assisted with reinforcement details as well as a review of the manuscript for this paper. The author also appreciates the efforts of BERGER/ABAM Engineers, Inc., in particular Jim Guarre, Warren Wilson, and Michelle Tragesser, for taking on the final detailed engineering and drafting of the Standard Plans. Thanks are also extended to Paul Bott of Sverdrup/DeLeuw for information of the Salt Lake City I-15 project.

From industry, thanks are extended to Doug Buss of V. Van Dyke, Inc. and Don Taylor Jr. of T & T Trucking, Inc. for their help in establishing the feasibility of shipping the new girder sections. Karsten Olson of Max J. Kuney Co. and Mark Johnnie of Atkinson Construction Co. helped to establish that there are no "fatal flaws" in WSDOT's conceptual design of the Methow and Twisp Bridges.

## REFERENCES

1. Bardow, A. K., Seraderian, R. L., and Culmo, M. P., "Design, Fabrication, and Construction of the New England Bulb-Tee Girder," *PCI JOURNAL*, V. 42, No. 6, November-December 1997, pp. 30-40.
2. Abdel-Karim, A. M., and Tadros, M. K., *State-of-the-Art of Precast/Prestressed Concrete Spliced I-Girder Bridges*, Precast/Prestressed Concrete Institute, Chicago, IL, October 1992.
3. AASHTO, *LRFD Bridge Design Specifications*, First Edition, American Association of State Highway and Transportation Officials, Washington, D.C., 1994.
4. Geren, K. L., and Tadros, M. K., "The NU Precast/Prestressed Concrete Bridge I-Girder Series," *PCI JOURNAL*, V. 39, No. 3, May-June 1994, pp. 26-39.
5. ACI Committee 318, "Building Code Requirements for Structural Concrete (ACI 318-95)," American Concrete Institute, Farmington Hills, MI, 1995.
6. Guyon, Y., *Prestressed Concrete*, V. 1, Jointly published by Contractors Record Ltd., London, United Kingdom, and John Wiley & Sons, Inc., New York, NY, 1953, p. 239.
7. Aswad, A., "An Efficiency Criterion for Pretensioned I-Girders" (unpublished).
8. Rabbat, B. G., and Russell, H. G., "Optimized Sections for Precast Prestressed Bridge Girders," *PCI JOURNAL*, V. 27, No. 4, July-August 1982, pp. 88-104.
9. PCI Committee on Prestress Losses, "Recommendations for Estimating Prestress Losses," *PCI JOURNAL*, V. 20, No. 4, July-August 1975, pp. 43-75.
10. Seguirant, S. J., and Anderson, R. G., "Prestress Losses (Phase I)," Concrete Technology Associates Technical Bulletin 84B2, April 1985.
11. ACI-ASCE Committee 423, "Tentative Recommendations for Prestressed Concrete," *ACI Journal*, V. 54, No. 7, January 1958, pp. 545-578.
12. Pessiki, S., Kaczinski, M., and Wescott, H. H., "Evaluation of Effective Prestress Force in 28-Year-Old Prestressed Concrete Bridge Beams," *PCI JOURNAL*, V. 41, No. 6, November-December 1996, pp. 78-89.
13. Rabbat, B. G., "25-Year-Old Prestressed Concrete Bridge Girders Tested," *PCI JOURNAL*, V. 29, No. 1, January-February 1984, pp. 177-179.
14. Shenoy, C. V., and Frantz, G. C., "Structural Tests of 27-Year-Old Prestressed Concrete Bridge Beams," *PCI JOURNAL*, V. 36, No. 5, September-October 1991, pp. 80-90.
15. AASHTO, *Standard Specifications for Highway Bridges*, Sixteenth Edition, American Association of State Highway and Transportation Officials, Washington, D.C., 1996.
16. *PCI Bridge Design Manual*, Precast/Prestressed Concrete Institute, Chicago, IL, 1997.
17. Mast, R. F., "Lateral Stability of Long Prestressed Concrete Beams, Part 1," *PCI JOURNAL*, V. 34, No. 1, January-February 1989, pp. 34-53.
18. Mast, R. F., "Lateral Stability of Long Prestressed Concrete Beams, Part 2," *PCI JOURNAL*, V. 38, No. 1, January-February 1993, pp. 70-88.
19. Imper, R. R., and Laszlo, G., "Handling and Shipping of Long Span Bridge Beams," *PCI JOURNAL*, V. 32, No. 6, November-December 1987, pp. 86-101.
20. AASHTO, *Guide Specifications for Design and Construction of Segmental Concrete Bridges*, American Association of State Highway and Transportation Officials, Washington, D.C., 1989.

## APPENDIX A — NOTATION

<p> <math>a_l</math> = length of overhang for lifting  <math>a_t</math> = length of overhang for trucking  <math>A_c</math> = gross concrete area of beam  <math>A_s</math> = area of one prestressing strand  <math>b</math> = distance from end of beam to harp point  <math>b_b</math> = bottom flange width  <math>b_t</math> = top flange width  <math>d_v</math> = effective shear depth  <math>e</math> = eccentricity of prestress force  <math>e_e</math> = eccentricity of prestress force at end of beam  <math>e_h</math> = eccentricity of prestress force at harp point  <math>e_i</math> = initial eccentricity of center of gravity of beam  <math>e_{lift}</math> = lateral placement tolerance for lifting device  <math>e_s</math> = eccentricity of prestress force at support  <math>e_{sweep}</math> = sweep tolerance for beam  <math>e_{truck}</math> = lateral placement tolerance on truck support  <math>e' = e_h - e_e</math>  <math>E_c</math> = modulus of elasticity of concrete at design strength  <math>E_{ci}</math> = modulus of elasticity of concrete at release strength  <math>f_b</math> = bottom fiber stress  <math>f'_c</math> = concrete cylinder strength at time of handling or shipping  <math>f'_{ci}</math> = initial concrete cylinder strength at time of release of prestress  <math>f_{po}</math> = initial jacking stress  <math>f_r</math> = modulus of rupture of concrete  <math>f_{si}</math> = effective stress in strand immediately after release of prestress  <math>f_{ss}</math> = effective stress in strand at time of shipping  <math>f_t</math> = top fiber stress  <math>F_{offset}</math> = offset factor that determines distance between roll axis and center of gravity of arc of curved beam  <math>FS</math> = factor of safety against cracking  <math>FS'</math> = factor of safety against failure  <math>h</math> = overall depth of beam  <math>h_{cg}</math> = height of center of gravity of beam above road  <math>h_r</math> = height of roll center above road  <math>I</math> = gross major axis moment of inertia of beam  <math>I</math> = impact during shipping  <math>I_{eff}</math> = effective cracked section minor axis (lateral) moment of inertia  <math>I_y</math> = gross minor axis (lateral) moment of inertia of beam  <math>K_\theta</math> = sum of rotational spring constants of supports  <math>l_g</math> = overall length of beam  <math>l_l</math> = length between lifting devices  <math>l_{span}</math> = span length, center-to-center of bearings  <math>l_t</math> = length between truck supports  <math>M</math> = moment                 </p>	<p> <math>M_h</math> = self-weight bending moment of beam at harp point  <math>M_{lat}</math> = lateral bending moment at cracking  <math>M_s</math> = self-weight bending moment of beam at support  <math>N</math> = number of prestressing strands  <math>P_i</math> = initial prestressing force after release of prestress  <math>P_s</math> = prestressing force at time of shipping  <math>r</math> = radius of gyration = <math>\sqrt{I/A_c}</math>  <math>r</math> = radius of stability = <math>K_\theta/W</math>  <math>S_b</math> = bottom section modulus  <math>S_t</math> = top section modulus  <math>w</math> = weight per unit length of beam  <math>w_c</math> = unit weight of concrete (for elastic modulus calculations)  <math>W</math> = total weight of beam  <math>x</math> = distance from support to harp point  <math>y</math> = height of center of gravity of beam above roll axis (beam supported from below)  <math>y_b</math> = height from bottom of beam to centroid of concrete section  <math>y_r</math> = height of roll axis above center of gravity of beam (hanging beam)  <math>y_t</math> = height from top of beam to centroid of concrete section  <math>\bar{z}</math> = lateral deflection of center of gravity of beam  <math>z_{max}</math> = distance from centerline of vehicle to center of dual tires  <math>\bar{z}_o</math> = theoretical lateral deflection of center of gravity of beam with full dead weight applied laterally  <math>\bar{z}'_o</math> = theoretical lateral deflection of center of gravity of beam with full dead weight applied laterally, computed using <math>I_{eff}</math> for tilt angle <math>\theta</math> under consideration  <math>\alpha</math> = Aswad efficiency ratio  <math>\alpha</math> = superelevation angle, or tilt angle of support  <math>\gamma_c</math> = unit weight of concrete including reinforcement (for weight calculations)  <math>\Delta</math> = total camber  <math>\Delta_{ohang}</math> = additional component of upward deflection due to overhangs  <math>\Delta_{ps}</math> = component of upward deflection due to prestress  <math>\Delta_{self}</math> = component of downward deflection due to self-weight  <math>\theta</math> = roll angle of major axis of beam with respect to vertical  <math>\theta_i</math> = initial roll angle of a rigid beam = <math>e_i/y_r</math>  <math>\theta_{max}</math> = tilt angle at which cracking begins  <math>\theta'_{max}</math> = tilt angle at maximum factor of safety against failure  <math>\rho</math> = Guyon efficiency factor                 </p>
---	---

## APPENDIX B — DIMENSIONS AND SECTION PROPERTIES OF NEW WSDOT STANDARD SECTIONS

Dimensions in millimeters.

Designation	D1	D2	D3	D4	D5	D6	D7	D8	B1	B2	B3
W21MG	2100	75	75	75	1555	75	115	130	1245	975	155
W24MG	2400	75	75	75	1855	75	115	130	1245	975	155
W21PTMG	2100	75	75	75	1555	75	115	130	1290	1020	200
W24PTMG	2400	75	75	75	1855	75	115	130	1290	1020	200

Dimensions in inches.

Designation	D1	D2	D3	D4	D5	D6	D7	D8	B1	B2	B3
W21MG	82.68	2.95	2.95	2.95	61.22	2.95	4.53	5.12	49.02	38.39	6.10
W24MG	94.49	2.95	2.95	2.95	73.03	2.95	4.53	5.12	49.02	38.39	6.10
W21PTMG	82.68	2.95	2.95	2.95	61.22	2.95	4.53	5.12	50.79	40.16	7.87
W24PTMG	94.49	2.95	2.95	2.95	73.03	2.95	4.53	5.12	50.79	40.16	7.87

Section properties in S.I. units.

Designation	A (mm <sup>2</sup> )	I (mm <sup>4</sup> )	y <sub>b</sub> (mm)	y <sub>t</sub> (mm)	S <sub>b</sub> (mm <sup>3</sup> )	S <sub>t</sub> (mm <sup>3</sup> )	w (kN/m)	I <sub>y</sub> (mm <sup>4</sup> )	V/S
W21MG	627096	3.981 × 10 <sup>11</sup>	1007	1093	3.951 × 10 <sup>8</sup>	3.643 × 10 <sup>8</sup>	15.76	2.993 × 10 <sup>10</sup>	3.16
W24MG	673547	5.504 × 10 <sup>11</sup>	1153	1247	4.775 × 10 <sup>8</sup>	4.412 × 10 <sup>8</sup>	16.93	3.003 × 10 <sup>10</sup>	3.15
W21PTMG	721289	4.329 × 10 <sup>11</sup>	1013	1087	4.274 × 10 <sup>8</sup>	3.982 × 10 <sup>8</sup>	18.13	3.462 × 10 <sup>10</sup>	3.59
W24PTMG	781289	6.023 × 10 <sup>11</sup>	1159	1241	5.196 × 10 <sup>8</sup>	4.855 × 10 <sup>8</sup>	19.64	3.482 × 10 <sup>10</sup>	3.61

Section properties in U.S. Customary units.

Designation	A (sq in.)	I (in. <sup>4</sup> )	y <sub>b</sub> (in.)	y <sub>t</sub> (in.)	S <sub>b</sub> (cu in.)	S <sub>t</sub> (cu in.)	w (kips per lineal ft)	I <sub>y</sub> (in. <sup>4</sup> )	V/S
W21MG	972	956,329	39.66	43.02	24,113	22,231	1.08	71,914	3.16
W24MG	1044	1,322,223	45.38	49.11	29,137	26,925	1.16	72,138	3.15
W21PTMG	1118	1,040,022	39.88	42.80	26,079	24,301	1.24	83,173	3.59
W24PTMG	1211	1,447,119	45.64	48.85	31,707	29,625	1.35	83,653	3.61

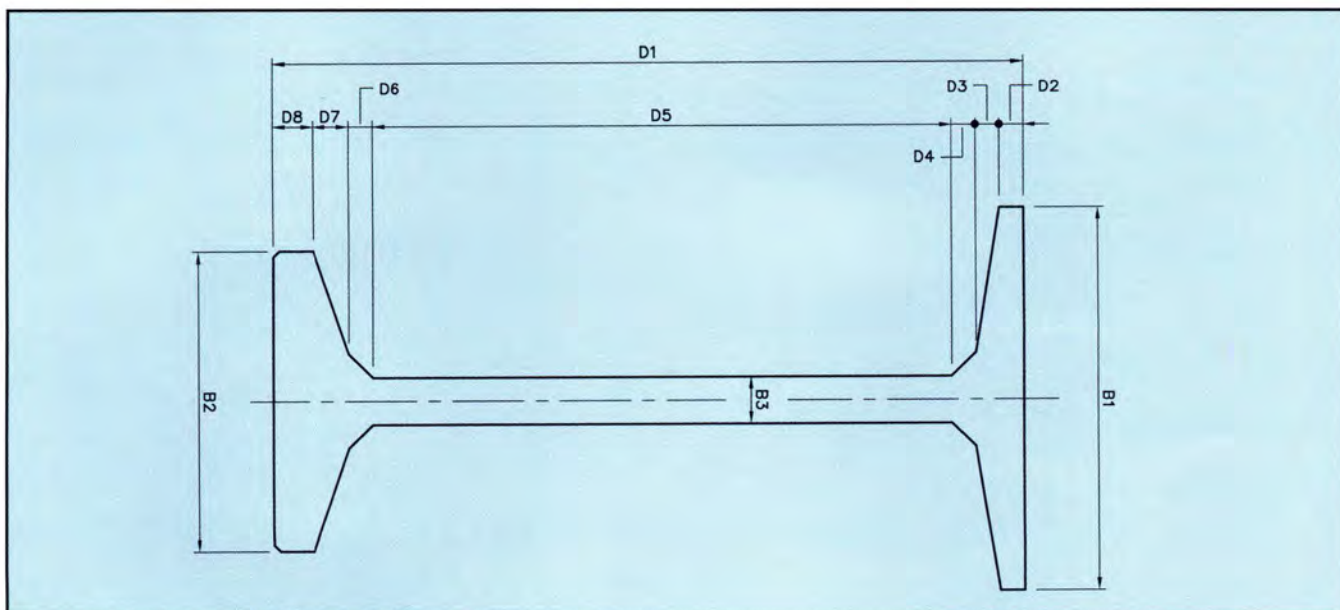


Fig. B1. Notation for dimensions contained in tables.





## APPENDIX D — SAMPLE CALCULATIONS

This sample calculation is based on the longest W21MG section with the highest level of pretensioning that can be manufactured in the Pacific Northwest. It is also based on calculation procedures given by Mast,<sup>17,18</sup> and bracing methods given by Imper and Laszlo.<sup>19</sup> See those references for additional details.

### GIVEN

#### W21MG Bridge Girder Data

Overall length of girder	$l_g = 185 \text{ ft (56.39 m)}$
Clear span length, center-to-center supports	$l_{span} = 182 \text{ ft (55.47 m)}$
Overall depth of girder	$h = 82.68 \text{ in. (2100 mm)}$
Top flange width	$b_t = 49.02 \text{ in. (1245 mm)}$
Bottom flange width	$b_b = 38.39 \text{ in. (975 mm)}$
Gross concrete area of girder cross section	$A_c = 972 \text{ sq in. (627096 mm}^2\text{)}$
Major axis moment of inertia	$I = 956,329 \text{ in.}^4 \text{ (3.981} \times 10^{11} \text{ mm}^4\text{)}$
Major axis top section modulus	$S_t = 22,230 \text{ cu in. (3.643} \times 10^8 \text{ mm}^3\text{)}$
Major axis bottom section modulus	$S_b = 24,113 \text{ cu in. (3.951} \times 10^8 \text{ mm}^3\text{)}$
Minor axis moment of inertia	$I_y = 71,914 \text{ in.}^4 \text{ (2.993} \times 10^{10} \text{ mm}^4\text{)}$
Distance from center of gravity of concrete to girder top	$y_t = 43.02 \text{ in. (1093 mm)}$
Distance from center of gravity of concrete to girder bottom	$y_b = 39.66 \text{ in. (1007 mm)}$
Girder weight per unit length	$w = 1.080 \text{ kip/ft (15.76 kN/m)}$
Girder weight	$W = 199.8 \text{ kips (888.8 kN)}$

#### Girder Concrete Data

Design strength	$f'_c = 10.0 \text{ ksi (68.95 MPa)}$
Unit weight including reinforcement	$\gamma_c = 160 \text{ pcf (25.13 kN/m}^3\text{)}$
Unit weight for elastic modulus calculations	$w_c = 155 \text{ pcf (24.35 kN/m}^3\text{)}$

#### Pretensioning Data

See Fig. D2 for pretensioning configuration	
Area of one 0.6 in. (15 mm) diameter strand	$A_s = 0.217 \text{ sq in. (140 mm}^2\text{)}$
Number of 0.6 in. (15 mm) diameter strands	$N = 64$
Initial jacking stress	$f_{po} = 202.5 \text{ ksi (1396 MPa)}$
Per WSDOT's Standard Specifications:	
Effective prestress at 1 day to 1 month (stripping)	$f_{si} = 182.5 \text{ ksi (1258 MPa)}$
Effective prestress at 1 month to 1 year (shipping)	$f_{ss} = 167.5 \text{ ksi (1155 MPa)}$

#### Lifting and Shipping Parameters

See Fig. D1 for lifting and shipping configurations	
Superelevation angle	$\alpha = 6 \text{ percent}$
Impact during shipping	$I = 20 \text{ percent}$
Sweep tolerance (shipping)	$e_{sweep} = 50 \text{ percent PCI tolerance}$
Sweep tolerance (shipping)	$e_{sweep} = 100 \text{ percent PCI tolerance}$
Lift device tolerance	$e_{lift} = 0.25 \text{ in. (6.4 mm)}$
Position tolerance on truck	$e_{truck} = 1 \text{ in. (25.4 mm)}$
Truck rotational spring stiffness	$K_\theta = 41,000 \text{ kip-in./rad (4632 kN-m/rad)}$
Height of roll center above road	$h_r = 24 \text{ in. (610 mm)}$
Height of center of gravity of girder above road	$h_{cg} = 111.7 \text{ in. (2837 mm)}$
Distance from center of truck to center of dual tires	$z_{max} = 36 \text{ in. (914 mm)}$

### REQUIRED

#### 1. Find lifting device location:

From Fig. 21 for a girder length of 185 ft (56.39 m) with 64 strands, the lifting device location can be extrapolated at approximately 14 ft (4.27 m). (This is a hypothetical exam-

ple of a worst case scenario, so the plotted point falls outside the bounds of the chart.)

$$a_l = 14 \text{ ft (4.27 m)}$$

$$l_l = 157 \text{ ft (47.85 m)}$$

$$x = b - a_l = 74.3 - 14 = 60.3 \text{ ft (18.38 m)}$$

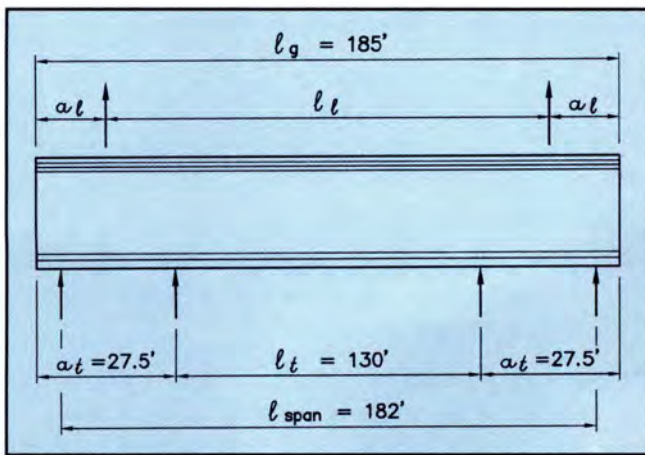


Fig. D1. Locations of bearing, lifting devices and truck supports.

## 2. Check stresses at harp point and support, and determine required concrete release strength:

$$f_t = \frac{P_i}{A_c} - \frac{P_i e}{S_t} + \frac{M}{S_t}$$

$$f_b = \frac{P_i}{A_c} + \frac{P_i e}{S_b} - \frac{M}{S_b}$$

$$P_i = N A_s f_{si} = (64)(0.217)(182.5) = 2535 \text{ kips (11274 kN)}$$

$$e_h = 35.52 \text{ in. (902 mm)}$$

$$e_s = 16.29 + \frac{19.23}{74.3}(14) = 19.91 \text{ in. (506 mm)}$$

$$M_h = \frac{w}{2}(l_1 x - x^2 - a_1^2) = \frac{1.08}{2}[(157)(60.3) - (60.3)^2 - (14)^2](12) = 36,515 \text{ kip-in. (4126 kN-m)}$$

$$M_s = \frac{w a_1^2}{2} = -\frac{(1.08)(14)^2(12)}{2} = -1270 \text{ kip-in. (-144 kN-m)}$$

At harp point:

$$f_t = \frac{2535}{972} - \frac{(2535)(35.52)}{22,230} + \frac{36,515}{22,230} = 0.200 \text{ ksi (1.38 MPa)}$$

$$r = \frac{K_\theta}{W} = \frac{41,000}{199.8} = 205.21 \text{ in. (5212 mm)}$$

At support:

$$f_t = \frac{2535}{972} - \frac{(2535)(19.91)}{22,230} + \frac{-1270}{22,230} = 0.280 \text{ ksi (1.93 MPa)}$$

$$f_b = \frac{2535}{972} + \frac{(2535)(19.91)}{24,113} - \frac{-1270}{24,113} = 4.754 \text{ ksi (32.78 MPa)}$$

Compression in the bottom flange at the harp point governs:

$$f'_{ci} = \frac{f_b}{0.6} = \frac{4.828}{0.6} = 8.047 \text{ ksi}$$

Use  $f'_{ci} = 8.10 \text{ ksi (55.5 MPa)}$

$$E_{ci} = 33w_c^{1.5} \sqrt{f'_{ci}} = \frac{33(155)^{1.5} \sqrt{8100}}{1000} = 5731 \text{ ksi (39518 MPa)}$$

Note: Compression in the bottom flange at the harp point exceeds compression in the bottom flange at the support. At this point, the location where the harped strands exit the girder end could be lowered to make these stresses roughly equivalent. This would not change the required concrete release strength, and would reduce the demand on the pretensioning system.

## 3. Compute initial eccentricity $e_i$ :

$$e_{sweep} = \frac{1}{16} \left( \frac{185}{10} \right) = 1.16 \text{ in. (29.4 mm)}$$

$$\text{Offset factor} = F_{offset} = \left( \frac{l_1}{l_g} \right)^2 - \frac{1}{3} = \left( \frac{157}{185} \right)^2 - \frac{1}{3} = 0.387$$

$$e_{lift} = 0.25 \text{ in. (6.4 mm)}$$

$$e_i = 1.16(0.387) + 0.25 = 0.70 \text{ in. (17.8 mm)}$$

## 4. Estimate initial camber to correct $y$ , (PCI Design Handbook Method):

Precast downward deflection due to self weight:

$$\Delta_{self} = \frac{-5w l_g^4}{384 E_{ci} I} = \frac{-5(1.08)(185)^4(12)^3}{384(5731)(956,329)} = -5.19 \text{ in. (-132 mm)}$$

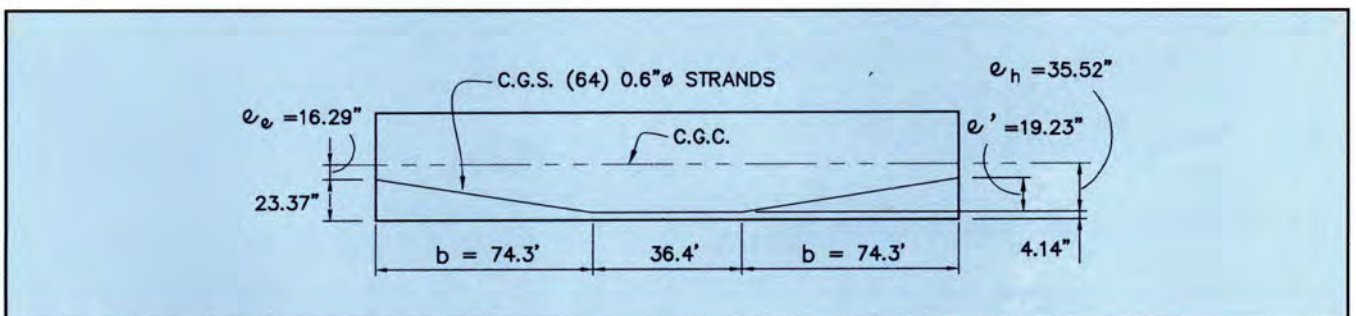


Fig. D2. Pretensioning configuration (without temporary top prestressing).



Upward deflection due to prestress:

$$\begin{aligned}\Delta_{ps} &= \frac{P_i e_e l_g^2}{8E_{ci}I} + \frac{P_i e' \left( \frac{l_g^2}{8} - \frac{b^2}{6} \right)}{E_{ci}I} \\ &= \frac{(2535)(16.29)(185)^2(12)^2}{8(5731)(956,329)} + \\ &\quad \frac{(2535)(19.23) \left[ \frac{(185)^2}{8} - \frac{(74.3)^2}{6} \right] (12)^2}{(5731)(956,329)} \\ &= 8.94 \text{ in. (227 mm)}\end{aligned}$$

Additional upward deflection due to overhang:

$$\begin{aligned}\Delta_{ohang} &= \frac{w a l_g^3}{16E_{ci}I} = \frac{(1.08)(14)(185)^3(12)^3}{16(5731)(956,329)} \\ &= 1.89 \text{ in. (47.9 mm)}\end{aligned}$$

Total camber at lifting:

$$\begin{aligned}\Delta &= \Delta_{self} + \Delta_{ps} + \Delta_{ohang} = -5.19 + 8.94 + 1.89 \\ &= 5.64 \text{ in. (143 mm)} \\ \text{Adjusted } y_r & \\ &= y_i - \Delta F_{offset} = 43.02 - (5.64)(0.387) \\ &= 40.84 \text{ in. (1037 mm)}\end{aligned}$$

5. Compute  $\bar{z}_o$ :

$$\begin{aligned}\bar{z}_o &= \frac{w}{12E_{ci}I_y l_g} \left( \frac{1}{10} l_i^5 - a_i^2 l_i^3 + 3a_i^4 l_i + \frac{6}{5} a_i^5 \right) \\ &= \frac{1.08}{12(5731)(71,914)(185)} \times \\ &\quad \left[ \frac{1}{10} (157)^5 - (14)^2 (157)^3 + 3(14)^4 (157) + \frac{6}{5} (14)^5 \right] (12)^5 \\ &= 17.95 \text{ in. (456 mm)}\end{aligned}$$

6. Compute  $\theta_i$ :

$$\theta_i = \frac{e_i}{y_r} = \frac{0.70}{40.84} = 0.01714$$

7. Compute tilt angle  $\theta_{max}$  at cracking:

$$\begin{aligned}f_r &= 7.5 \sqrt{f'_{ci}} = \frac{7.5 \sqrt{8100}}{1000} = 0.675 \text{ ksi (4.65 MPa)} \\ f_t &= 0.200 \text{ ksi (1.38 MPa) compression from Step 2} \\ M_{lar} &= \frac{2(f_r + f_t)I_y}{b_t} = \frac{2(0.675 + 0.200)(71,914)}{49.02} \\ &= 2567 \text{ kip-in. (290 kN-m)} \\ \theta_{max} &= \frac{M_{lar}}{M_h} = \frac{2567}{36,515} = 0.0703\end{aligned}$$

8. Compute factor of safety against cracking  $FS$ :

$$FS = \frac{1}{\frac{\bar{z}_o}{y_r} + \frac{\theta_i}{\theta_{max}}} = \frac{1}{\frac{17.95}{40.84} + \frac{0.01714}{0.0703}} = 1.46 > 1.0 \text{ (ok)}$$

9. Compute factor of safety against failure  $FS'$ :

$$\begin{aligned}\theta'_{max} &= \sqrt{\frac{e_i}{2.5\bar{z}_o}} = \sqrt{\frac{0.70}{2.5(17.95)}} = 0.1249 \\ \bar{z}'_o &= \bar{z}_o (1 + 2.5\theta'_{max}) = (17.95)[1 + 2.5(0.1249)] \\ &= 23.55 \text{ in. (598 mm)} \\ FS' &= \frac{y_r \theta'_{max}}{\bar{z}'_o \theta'_{max} + e_i} = \frac{(40.84)(0.1249)}{(23.55)(0.1249) + (0.70)} \\ &= 1.40 < 1.5\end{aligned}$$

If  $FS' < FS$ ,  $FS' = FS$ , therefore  $FS' = 1.46$ . This is within a few percent of the suggested factor of safety against failure and is probably satisfactory. If more stability is considered necessary, move the lifting devices a few more inches toward midspan and repeat Steps 2 through 9.

Check the same beam during transportation:

GIVEN

Local truckers prefer a maximum of 130 ft (39.62 m) between the centers of support of the tractor and trailer for turning radius purposes. Try  $l_t = 130$  ft (39.62 m),  $a_t = 27.5$  ft (8.38 m).

Fig. 24 indicates that girders of this size will need about five temporary top strands to maintain a factor of safety of 1.0 against cracking during shipping. Try six temporary top strands, jacked to the same level as the permanent pretensioning.

REQUIRED

10. Compute  $r$ :

$$r = \frac{K_\theta}{W} = \frac{41,000}{199.8} = 205.21 \text{ in. (5212 mm)}$$

11. Compute tilt angle  $\theta$ :

$y = h_{cg} - h_r = 111.70 - 24 = 87.70$  in. (2228 mm)  
Increase  $y$  by 2 percent to allow for camber. Then,  $y = 89.45$  in. (2272 mm).

$$F_{offset} = \left( \frac{l_t}{l_g} \right)^2 - \frac{1}{3} = \left( \frac{130}{185} \right)^2 - \frac{1}{3} = 0.160$$

$$e_{sweep} = \frac{1}{8} \left( \frac{185}{10} \right) = 2.31 \text{ in. (58.7 mm)}$$

$$e_{truck} = 1 \text{ in. (25.4 mm)}$$

$$e_i = (0.160)(2.31) + 1 = 1.37 \text{ in. (34.8 mm)}$$

$$\begin{aligned}E_c &= 33w_c^{1.5} \sqrt{f'_c} = \frac{33(155)^{1.5} \sqrt{10,000}}{1000} \\ &= 6368 \text{ ksi (43907 MPa)}\end{aligned}$$

$$\begin{aligned}\bar{z}_o &= \frac{w}{12E_{ci}I_y l_g} \left( \frac{1}{10} l_i^5 - a_i^2 l_i^3 + 3a_i^4 l_i + \frac{6}{5} a_i^5 \right) \\ &= \frac{1.08(12)^3}{12(6368)(71,914)(185)} \times \\ &\quad \left[ \frac{1}{10} (130)^5 - (27.5)^2 (130)^3 + 3(27.5)^4 (130) + \frac{6}{5} (27.5)^5 \right]\end{aligned}$$

$$\left[ \frac{1}{10} (130)^5 - (27.5)^2 (130)^3 + 3(27.5)^4 (130) + \frac{6}{5} (27.5)^5 \right]$$

$$= 4.21 \text{ in. (107 mm)}$$

$$\theta = \frac{ar + e_i}{r - y - \bar{z}_o} = \frac{(0.06)(205.21) + 1.37}{205.21 - 89.45 - 4.21} = 0.1227$$

**12. Compute stresses of tilted girder at harp point (no impact):**

$$P_s = N A_s f_{ss} = (70)(0.217)(167.5) = 2544 \text{ kips (11317 kN)}$$

$$e_h = \frac{(64)(35.52) - (6)(43.02 - 1.97)}{70} = 28.96 \text{ in. (736 mm)}$$

$$M_h = \frac{w}{2} (l_t x - x^2 - a_t^2) = \frac{1.08}{2} [(130)(46.8) - (46.8)^2 - (27.5)^2] (12) = 20,331 \text{ kip-in. (2297 kN-m)}$$

$$f_t = \frac{2544}{972} - \frac{(2544)(28.96)}{22,230} + \frac{20,331}{22,230} = 0.218 \text{ ksi (1.50 MPa)}$$

$$f_b = \frac{2544}{972} + \frac{(2544)(28.96)}{24,113} - \frac{20,331}{24,113} = 4.830 \text{ ksi (33.30 MPa)}$$

$$M_{lat} = \theta M_h = 0.1227(20,331) = 2494 \text{ kip-in. (281.8 kN-m)}$$

Top fiber stress for "uphill" flange:

$$f_t + \frac{M_{lat} \left( \frac{b_t}{2} \right)}{I_y} = 0.218 + \frac{2494 \left( \frac{49.02}{2} \right)}{71,914} = 1.068 \text{ ksi (7.36 MPa)}$$

Top fiber stress for "downhill" flange:

$$f_t - \frac{M_{lat} \left( \frac{b_t}{2} \right)}{I_y} = 0.218 - \frac{2494 \left( \frac{49.02}{2} \right)}{71,914} = -0.632 \text{ ksi (-4.36 MPa)}$$

Bottom fiber stress for "uphill" flange:

$$f_b + \frac{M_{lat} \left( \frac{b_b}{2} \right)}{I_y} = 4.830 + \frac{2494 \left( \frac{38.39}{2} \right)}{71,914} = 5.496 \text{ ksi (37.89 MPa)}$$

Bottom fiber stress for "downhill" flange:

$$f_b - \frac{M_{lat} \left( \frac{b_b}{2} \right)}{I_y} = 4.830 - \frac{2494 \left( \frac{38.39}{2} \right)}{71,914} = 4.165 \text{ ksi (28.71 MPa)}$$

Compression in "uphill" bottom flange governs:

$$f'_c = \frac{f_b}{0.6} = \frac{5.496}{0.6} = 9.160 \text{ ksi (63.16 MPa)} < 10.0 \text{ ksi (68.95 MPa)} \text{ (ok)}$$

Tension in "downhill" top flange governs

$$f'_c = \left( \frac{f_t}{7.5} \right)^2 = \left( \frac{632}{7.5} \right)^2 = 7101 \text{ psi} = 7.101 \text{ ksi (48.96 MPa)} < 10.0 \text{ ksi (ok)}$$

**13. Compute stresses including impact (required by the WSDOT Standard Specifications):**

Stresses at harp point with +20 percent impact:

$$f_t = \frac{2544}{972} - \frac{(2544)(28.96)}{22,230} + \frac{(20,331)(1.2)}{22,230} = 0.400 \text{ ksi (2.76 MPa)}$$

$$f_b = \frac{2544}{972} + \frac{(2544)(28.96)}{24,113} - \frac{(20,331)(1.2)}{24,113} = 4.661 \text{ ksi (32.14 MPa)}$$

Stresses at harp point with -20 percent impact:

$$f_t = \frac{2544}{972} - \frac{(2544)(28.96)}{22,230} + \frac{(20,331)(0.8)}{22,230} = 0.035 \text{ ksi (0.24 MPa)}$$

$$f_b = \frac{2544}{972} + \frac{(2544)(28.96)}{24,113} - \frac{(20,331)(0.8)}{24,113} = 4.999 \text{ ksi (34.47 MPa)}$$

Stresses at support with +20 percent impact:

$$e_s = \frac{\left[ 16.29 + \frac{19.23}{74.3} (27.5) \right] 64 - (43.02 - 1.97) 6}{70} = 17.88 \text{ in. (454 mm)}$$

$$M_s = \frac{w a_t^2}{2} = -\frac{(1.08)(27.5)^2 (12)}{2} = -4900 \text{ kip-in. (-554 kN-m)}$$

$$f_t = \frac{2544}{972} - \frac{(2544)(17.88)}{22,230} + \frac{(-4900)(1.2)}{22,230} = 0.306 \text{ ksi (2.11 MPa)}$$

$$f_b = \frac{2544}{972} + \frac{(2544)(17.88)}{24,113} - \frac{(-4900)(1.2)}{24,113} = 4.748 \text{ ksi (32.74 MPa)}$$

Stresses at support with -20 percent impact:

$$f_t = \frac{2544}{972} - \frac{(2544)(17.88)}{22,230} + \frac{(-4900)(0.8)}{22,230} = 0.395 \text{ ksi (2.72 MPa)}$$

$$f_b = \frac{2544}{972} + \frac{(2544)(17.88)}{24,113} - \frac{(-4900)(0.8)}{24,113} = 4.667 \text{ ksi (32.18 MPa)}$$

Compression in bottom flange at harp point with -20 percent impact governs:

$$f'_c = \frac{f_b}{0.6} = \frac{4.999}{0.6} = 8.331 \text{ ksi (57.44 MPa)} < 10.0 \text{ ksi (68.95 MPa)} \text{ (ok)}$$

**14. Compute the tilt angle  $\theta_{max}$  at cracking:**

$$f_r = 7.5\sqrt{f'_c} = \frac{7.5\sqrt{10,000}}{1000} = 0.750 \text{ ksi (5.17 MPa)}$$

$$f_t = 0.218 \text{ ksi (1.50 MPa) compression from Step 12}$$

$$M_{lat} = \frac{2(f_r + f_t)I_y}{b_t} = \frac{2(0.750 + 0.218)(71,914)}{49.02}$$

$$= 2840 \text{ kip-in. (321 kN-m)}$$

$$\theta_{max} = \frac{M_{lat}}{M_h} = \frac{2840}{20,331} = 0.1397$$

**15. Compute factor of safety against cracking  $FS$ :**

$$FS = \frac{r(\theta_{max} - \alpha)}{\bar{z}_o\theta_{max} + e_i + y\theta_{max}}$$

$$= \frac{205.21(0.1397 - 0.06)}{(4.21)(0.1397) + (1.37) + (89.45)(0.1397)}$$

$$= 1.13 > 1.0 \text{ (ok)}$$

**16. Compute tilt angle  $\theta'_{max}$  at maximum resisting arm:**

$$\theta'_{max} = \frac{z_{max} - h_r\alpha}{r} + \alpha = \frac{36 - (24)(0.06)}{205.21} + 0.06$$

$$= 0.2284$$

**17. Compute  $\bar{z}'_o$  at  $\theta'_{max}$ :**

$$\bar{z}'_o = \bar{z}_o(1 + 2.5\theta'_{max}) = 4.21[1 + 2.5(0.2284)]$$

$$= 6.61 \text{ in. (168 mm)}$$

**18. Compute factor of safety against rollover  $FS'$ :**

$$FS' = \frac{r(\theta'_{max} - \alpha)}{(\bar{z}'_o\theta'_{max} + e_i + y\theta'_{max})}$$

$$= \frac{205.21(0.2284 - 0.06)}{[(6.61)(0.2284) + 1.37 + (89.45)(0.2284)]}$$

$$= 1.48 \approx 1.50 \text{ (ok)}$$

**Check lateral stability and required concrete strength at release if the temporary top prestressing is introduced prior to stripping:**

**19. Find lifting device location:**

From Fig. 22 for a girder length of 185 ft (56.39 m) with 64 strands, the lifting device location can be extrapolated at somewhere between 11 and 13 ft (3.35 and 3.96 m). This chart is for four top strands, and six are used here, so the result is not directly applicable. Assume the lifting devices are 12.5 ft (3.81 m) from the ends of the girder as a reasonably conservative estimate.

$$a_l = 12.5 \text{ ft (3.81 m)}$$

$$l_l = 160 \text{ ft (47.85 m)}$$

$$x = 74.3 - 12.5 = 61.8 \text{ ft (18.84 m)}$$

**20. Check stresses at harp point and support, and determine required concrete release strength:**

$$P_i = (70)(0.217)(182.5) = 2772 \text{ kips (12331 kN)}$$

$$e_h = \frac{(64)(35.52) - (6)(43.02 - 1.97)}{70}$$

$$= 28.96 \text{ in. (736 mm)}$$

$$e_s = \frac{\left[16.29 + \frac{19.23}{74.3}(12.5)\right](64) - (43.02 - 1.97)6}{70}$$

$$= 14.33 \text{ in. (364 mm)}$$

$$M_h = \frac{1.08}{2} \left[ (160)(61.8) - (61.8)^2 - (12.5)^2 \right] (12)$$

$$= 38,313 \text{ kip-in. (4329 kN-m)}$$

$$M_s = -\frac{(1.08)(12.5)^2(12)}{2}$$

$$= -1012 \text{ kip-in. (-114 kN-m)}$$

At harp point:

$$f_t = \frac{2772}{972} - \frac{(2772)(28.96)}{22,230} + \frac{38,313}{22,230}$$

$$= 0.964 \text{ ksi (6.65 MPa)}$$

$$f_b = \frac{2772}{972} + \frac{(2772)(28.96)}{24,113} - \frac{38,313}{24,113}$$

$$= 4.593 \text{ ksi (31.67 MPa)}$$

At support:

$$f_t = \frac{2772}{972} - \frac{(2772)(14.33)}{22,230} + \frac{-1012}{22,230}$$

$$= 1.019 \text{ ksi (7.03 MPa)}$$

$$f_b = \frac{2772}{972} + \frac{(2772)(14.33)}{24,113} - \frac{-1012}{24,113}$$

$$= 4.541 \text{ ksi (31.31 MPa)}$$

Compression in the bottom flange at the harp point governs:

$$f'_{ci} = \frac{4.593}{0.6} = 7.655 \text{ ksi}$$

Use  $f'_{ci} = 7.70 \text{ ksi (53.1 MPa)}$

$$E_{ci} = \frac{33(155)^{1.5}\sqrt{7700}}{1000} = 5588 \text{ ksi (38530 MPa)}$$

**21. Re-compute initial eccentricity  $e_i$ :**

$$e_{sweep} = \frac{1}{16} \left( \frac{185}{10} \right) = 1.16 \text{ in. (29.4 mm)}$$

$$\text{Offset factor} = F_{offset} = \left( \frac{160}{185} \right)^2 - \frac{1}{3} = 0.415$$

$$e_{lift} = 0.25 \text{ in. (6.4 mm)}$$

$$e_i = 1.16(0.415) + 0.25 = 0.73 \text{ in. (18.6 mm)}$$

**22. Re-estimate initial camber to correct  $y_r$  (PCI****Design Handbook Method):**

Precast downward deflection due to self weight:

$$\Delta_{self} = \frac{-5(1.08)(185)^4(12)^3}{384(5588)(956239)} = -5.33 \text{ in. } (-135 \text{ mm})$$

$$e_e = \frac{(16.29)(64) - (43.02 - 1.97)6}{70}$$

$$= 11.38 \text{ in. } (289 \text{ mm})$$

$$e' = 28.96 - 11.38 = 17.58 \text{ in. } (447 \text{ mm})$$

Upward deflection due to prestress:

$$\Delta_{ps} = \frac{(2772)(11.38)(185)^2(12)^2}{8(5588)(956,329)} +$$

$$\frac{(2772)(17.58)}{(5588)(956,329)} \left[ \frac{(185)^2}{8} - \frac{(74.3)^2}{6} \right] (12)^2$$

$$= 8.05 \text{ in. } (204 \text{ mm})$$

Additional upward deflection due to overhang:

$$\Delta_{ohang} = \frac{(1.08)(12.5)(185)^3(12)^3}{16(5588)(956,329)} = 1.73 \text{ in. } (43.9 \text{ mm})$$

Total camber at lifting:

$$\Delta = -5.33 + 8.05 + 1.73 = 4.45 \text{ in. } (113 \text{ mm})$$

Adjusted  $y_r$

$$= 43.02 - (4.45)(0.415)$$

$$= 41.17 \text{ in. } (1046 \text{ mm})$$

**23. Re-compute  $\bar{z}_o$ :**

$$\bar{z}_o = \frac{1.08(12)^3}{12(5588)(71,914)(185)} \times$$

$$\left[ \frac{1}{10}(160)^5 - (12.5)^2(160)^3 + 3(12.5)^4(160) + \frac{6}{5}(12.5)^5 \right]$$

$$= 20.62 \text{ in. } (524 \text{ mm})$$

**24. Re-compute  $\theta_i$ :**

$$\theta_i = \frac{0.73}{41.17} = 0.0177$$

**25. Re-compute tilt angle  $\theta_{max}$  at cracking:**

$$f_r = \frac{7.5\sqrt{7700}}{1000} = 0.658 \text{ ksi } (4.54 \text{ MPa})$$

$$f_t = 0.964 \text{ ksi } (6.65 \text{ MPa}) \text{ compression from Step 20}$$

$$M_{lat} = \frac{2(0.658 + 0.964)(71,914)}{49.02}$$

$$= 4759 \text{ kip-in. } (538 \text{ kN-m})$$

$$\theta_{max} = \frac{4759}{38,313} = 0.1242$$

**26. Re-compute factor of safety against cracking  $FS$ :**

$$FS = \frac{1}{\frac{20.62}{41.17} + \frac{0.0177}{0.1242}} = 1.55 > 1.0 \text{ (ok)}$$

**27. Re-compute factor of safety against failure  $FS'$ :**

$$\theta_{max} = \sqrt{\frac{0.73}{2.5(20.62)}} = 0.1190$$

$$\bar{z}'_o = (20.62)[1 + 2.5(0.1190)] = 26.75 \text{ in. } (680 \text{ mm})$$

$$FS' = \frac{(41.17)(0.1190)}{(26.75)(0.1190) + (0.73)} = 1.25 < 1.5$$

If  $FS' < FS$ ,  $FS' = FS$ ; therefore,  $FS' = 1.55$ . The addition of temporary top prestressing before stripping reduces the required concrete release strength by approximately 400 psi (2.76 MPa) while improving the lateral stability factors of safety.